Theta burst stimulation in neglect after stroke: functional outcome and response variability origins

Thomas Nyffeler[a,b,c*], Tim Vanbellingen[a,b,c], Brigitte C. Kaufmann[b,c], Tobias Pflugshaupt[c], Daniel Bauer[c,], Julia Frey[c], Magdalena Chechlacz[d], Stephan Bohlhalter[c], René M. Müri[a,b], Tobias Nef[a], Dario Cazzoli[a,b]

[a]Gerontechnology and Rehabilitation Group, ARTORG Center for Biomedical Engineering Research University of Bern, Switzerland,

[b]Perception and Eye Movement Laboratory, Department of Neurology, University of Bern, Switzerland,

[c]Neurocenter, Luzerner Kantonsspital, Switzerland

[d]Centre for Human Brain Health, University of Birmingham

[*]Address for correspondence: Thomas Nyffeler, MD

Prof. Thomas Nyffeler, ARTORG Center for Biomedical Engineering Research, University of Bern, Bern, Switzerland.

E-mail address: thomas.nyffeler@luks.ch

ABSTRACT

Spatial neglect is a strong and negative predictor of general functional outcome after stroke, and its therapy remains a challenge. Whereas inhibitory non-invasive brain stimulation (NIBS) over the contralesional, intact hemisphere has generally been shown to ameliorate neglect on a group level, a conspicuous variability of the effects at the individual level is typically observed. We aimed to comprehensively assess the characteristics and determinants of the effects of inhibitory NIBS in neglect, identifying which patients would respond to this therapeutic approach and which not. To this end, we prospectively included sixty patients with a subacute right-hemispheric stroke. In thirty patients with spatial neglect, continuous Theta Burst Stimulation (cTBS) was applied over the left posterior parietal cortex (PPC) in a randomized clinical trial, either in 8 or 16 trains, or as sham stimulation. Thirty patients without neglect served as control group. Neglect severity was measured with a neuropsychological test battery and the Catherine Bergego Scale (CBS), at admission to and at discharge from inpatient neurorehabilitation, as well as at 3 months follow-up. General functional outcome was assessed by means of the Functional Independent Measurement (FIM) and the Lucerne ICF-based Multidisciplinary Observation Scale (LIMOS). The impact of clinical and demographic factors was evaluated, and the influence of lesion location and extension was assessed by means of voxel-based lesion-symptom mapping (VLSM). On a group level, both cTBS protocols (i.e., 8 and 16 trains) significantly reduced neglect severity in both the CBS and the neuropsychological tests, at discharge and 3 months later. Furthermore, cTBS significantly improved general functional outcome. On an individual level, hierarchical cluster and VLSM analyses revealed that the variability in the responses to cTBS is determined by the integrity of inter-hemispheric connections within the corpus callosum, in particular parieto-parietal connections. In cTBS responders, in whom neglect and general functional outcome were significantly improved, the corpus callosum was intact, whereas this was not the case in cTBS non-responders. Moreover, analyses based on the Proportional recovery rule and the Maugeri predictive stroke recovery model showed that the recovery

of neglect and of the activities of daily living (ADL) was accelerated only in cTBS responders. Furthermore, the level of ADL recovery of these neglect patients was brought close to the one of right-hemispheric control patients without neglect. Hence, in neglect patients with intact interhemispheric connectivity, cTBS over the contralesional PPC significantly improves and accelerates neglect recovery and, associated with it, general functional outcome.

Key words: spatial neglect, functional recovery, activities of daily living, right hemispheric stroke, non-invasive brain stimulation

ABBREVIATION LIST

ADL	activities of daily living
CBS	Catherine Bergego Scale
CoC	Center of Cancellation
CST	Corticospinal Tract
cTBS	continuous Theta Burst Stimulation
DTI	diffusion tensor imaging
FDR	False discovery rate
FIM	Functional Independent Measurement
JAMAR	Juvenile Arthritis Multidimensional Assessment Report
LIMOS	Lucerne ICF-based Multidisciplinary Observation Scale
LSD	least significant difference
MNI-space	coordinate system of the human brain developed by the Montreal Neurological Institute and Hospital
MoCA	Montreal Cognitive Assessment
NIBS	non-invasive brain stimulation
NIHSS	NIH Stroke Scale
NSA	Nottingham Sensory Assessment
PPC	posterior parietal cortex
RHD	right-hemispheric stroke
RHS	right-hemispheric stroke
SEM	standard error of the mean
SPT	smooth pursuit eye movement training
TMS	Transcranial Magnetic Stimulation
VLSM	voxel-based lesion-symptom mapping

INTRODUCTION

Amongst cognitive impairments after stroke, spatial neglect is very common, occurring in up to 43% of patients with a lesion of the right hemisphere (Ringman *et al.*, 2004). Spatial neglect severely affects the activities of daily living (ADL) and is a strong, negative, and independent predictor of general functional outcome (Nijboer *et al.*, 2013; Nijboer *et al.*, 2014). The relevance of the negative effects of spatial neglect on the long-term functional outcome in the ADL is further highlighted by the recently developed Maugeri predictive model of stroke outcome (Scrutinio *et al.*, 2017), which integrates the presence of spatial neglect as a main predictive factor.

The pathophysiological mechanisms underlying spatial neglect and its recovery are still controversial and debated. Some studies suggest a maladaptive role of the left, undamaged hemisphere, which undergoes a pathological hyperexcitability after a lesion of its contralateral homologue (Corbetta and Shulman, 2011; Kinsbourne, 1987). A reduction of this contralesional hyperexcitability has been typically targeted by inhibitory, non-invasive brain stimulation (NIBS), generally resulting in an amelioration of neglect symptoms on a group level (Salazar *et al.*, 2018). However, on an individual level, a conspicuous variability in the effects of contralesional, inhibitory NIBS in neglect has been observed, i.e., not all patients equally benefit from this approach (Lefaucheur et al., 2014). Conversely, and somewhat in line with this variability, some studies point to a compensatory role of the contralesional, undamaged hemisphere (Lunven *et al.*, 2015; Umarova *et al.*, 2016), suggesting that its activity should be facilitated rather than inhibited. Finally, in a third perspective, other recent studies have suggested that neglect recovery dynamics after stroke follow fixed, non-influenceable patterns: within three months after stroke, patients would recover ≈70% of their initial impairment, irrespectively of the type of applied therapeutic approaches (i.e., the so-called Proportional recovery rule, (Marchi *et al.*, 2017; Ramsey *et al.*, 2017; Winters *et al.*, 2017)).

The aim of the present study was to clarify these discrepancies between current perspectives. For this purpose, we assessed sixty patients with a subacute right-hemispheric stroke, who were prospectively recruited. Thirty of these patients presented with left-sided neglect, and were treated with continuous Theta Bust Stimulation (cTBS), an inhibitory, repetitive transcranial magnetic stimulation protocol (Huang *et al.*, 2005; Nyffeler *et al.*, 2006). cTBS was applied over the left posterior parietal cortex (PPC), a critical node of the dorsal attentional network (e.g., Corbetta and Shulman, 2011) in a randomized, double-blind, sham-controlled design. In order to assess a possible dose-response relationship, we applied either 8 or 16cTBS trains, and contrasted the results with the ones of sham stimulation. Neglect severity was assessed by means of the Catherine Bergego Scale (CBS) and a comprehensive neuropsychological test battery, at admission to and at discharge from inpatient neurorehabilitation, and at 3 months follow-up. In order to identify the determinants of the cTBS effects (i.e., in which patients an inhibition of the contralesional, left PPC would result in beneficial effects on neglect severity), we assessed the role of different patient characteristics such as demographic variables, clinical variables, and lesion localisation using voxel-based lesion-symptom mapping (VLSM). Moreover, in order to assess whether general functional outcome would be influenced by the cTBS intervention, we analysed recovery dynamics in the ADL, by measuring changes in the Functional Independence Measure (FIM) (Keith *et al.*, 1987) and in the Lucerne ICF-based Multidisciplinary Observation Scale (LIMOS) (Ottiger *et al.*, 2015; Vanbellingen *et al.*, 2016), and by quantifying the contribution of demographic and clinical factors. The results were systematically compared with those of the remaining thirty patients, who also suffered from a subacute right-hemispheric stroke, but did not present with neglect. Finally, we aimed at identifying patients whose recovery dynamics would fit the predictions of influential stroke recovery models (i.e., the Proportional recovery rule (Marchi *et al.*, 2017; Ramsey *et al.*, 2017; Winters *et al.*, 2017), and the Maugeri predictive model (Scrutinio *et al.*, 2017)), ascertaining whether cTBS would be able to positively influence the predicted outcome.

MATERIALS AND METHODS

Patients

Sixty patients (age 27-86 years, mean=66.4, SD=14.2; 24 women) with a first, right-hemispheric stroke (RHS) participated in the study. All patients were admitted to the Neurology and Neurorehabilitation Center, Luzerner Kantonsspital (LUKS), from April 2014 to February 2017, to receive multidisciplinary, inpatient neurorehabilitation, and were consecutively enrolled in the study (see the Consort diagram in the Supplementary Data for details).

Each patient underwent a full neurological examination at admission, including the NIH Stroke Scale (NIHSS). Hand grip strength of the affected upper limb was measured by means of the hydraulic hand dynamometer JAMAR (Chen *et al.*, 2009). Stereognosis was assessed by means of the corresponding subscale of the Nottingham Sensory Assessment (NSA) (Lincoln *et al.*, 1998). In addition, cognitive functioning was assessed by means of the Montreal Cognitive Assessment (MoCA) (Chiti and Pantoni, 2014). Thirty RHS patients presented with neglect and were randomized within the cTBS protocol. In order to estimate for the specific effects of neglect symptoms on functional outcome, thirty RHS patients without neglect served as a control group. The presence of neglect was defined as: a pathological score in the Catherine Bergego Scale (CBS; >=1), a mean relative rightward deviation from the actual midline of ≥ 11% in the Line Bisection Task (Schenkenberg *et al.*, 1980), and a Center of Cancellation (CoC) value of > 0.08 in the Bells test (Gauthier *et al.*, 1989; Rorden and Karnath, 2010). Patients suffering from major psychiatric disorders and other co-morbidities (i.e., drug and alcohol abuse) were excluded. In addition, for the patients undergoing the cTBS protocol, a history of epilepsy and the presence of metallic implants represented further exclusion criteria (Rossi *et al.*, 2009).

The randomisation procedure was carried out by a blinded collaborator (T.P.), using a computerized block randomisation protocol to ensure equal group sizes (https://www.random.org/integer-sets). Treatment allocation was concealed from the trained observers. The study followed the CONSORT guidelines and was conducted in accordance with

the principles laid down in the latest Declaration of Helsinki (WHO, 2013), and was approved by the local Ethics Committee of the state of Lucerne. All patients gave written informed consent prior to participation.

Lesion mapping and analysis

In order to identify the lesion-related determinants of the cTBS effects, lesion mapping, overlapping, volume determination, voxel-based lesion-symptom mapping (VLSM) analyses, and a probabilistic white matter fibre tract disconnection analysis were conducted with procedures similar to the ones described in our recent work (e.g.(Cazzoli *et al.*, 2016; Kaufmann *et al.*, 2018)). For a detailed description, please see the corresponding section in the Supplementary Methods.

Experimental procedures

All patients received interdisciplinary therapy in our neurorehabilitation clinic. In addition, all neglect patients also received smooth pursuit eye movement training (SPT), daily over a period of three weeks (for details concerning the precise SPT procedure, please see (Hopfner *et al.*, 2015)). All primary and secondary outcomes were assessed during the first week after admission to the clinic (henceforth referred to T0) and in the last week before discharge (henceforth referred to as T1). Neglect-related outcomes were additionally re-assessed in a follow-up testing session three months after discharge (henceforth referred to as T2).

Outcomes

Primary outcome

The CBS was chosen as the primary outcome measure, since this scale is particularly sensitive and has high ecological validity in the neglect rehabilitation context (Azouvi, 2017). The CBS quantifies the influence of spatial neglect-related deficits on the ADLs, assessing 10 activi-

ties of daily life, such as grooming, navigating, and exploring space. Each of the 10 items is scored on a 0-to-3 scale, with 0 indicating no neglect, and 3 indicating severe neglect (i.e., total CBS score range of 0–30). The CBS was completed by rehabilitation nurses taking care of the patients on a daily basis, who were blind with respect to the experimental protocol, and who observed the patients performing the different ADLs.

Secondary outcomes

A battery of several neuropsychological neglect tests was administered. Body representational neglect was assessed by means of the Fluff-test (Cocchini *et al.*, 2001), free visual exploration behaviour by means of the Two-Part-Picture-Test (Brunila *et al.*, 2003) in the near and far space, and visual search behaviour by means of the bird cancellation task (Hopfner *et al.*, 2015) (see Supplementary material).

Since inter- and intra-individual variability in the different neglect test results is typically high (Lundervold *et al.*, 2005), and a test battery is more sensitive than any single test alone (Azouvi *et al.*, 2002), a composite score was derived from the results of the single tests composing the above-mentioned battery. In order to aggregate the results of the different single tests, we first calculated standardized pre-post differences (Becker, 1988; Grawe and Braun, 1994) between admission and discharge (i.e., T0 and T1), and between discharge and follow up (i.e., T1 and T2), for each of the four test scores. We then calculated the mean of these four standardized scores, resulting in the composite score: $\left(composite\ score = \frac{\Sigma \frac{score_{pre} - score_{post}}{SD_{pre}}}{4} \right)$.

The general functional outcome was assessed by means of the FIM (Keith *et al.*, 1987) and of the LIMOS (Ottiger *et al.*, 2015). The LIMOS was included as an additional measure because it was shown to be more sensitive than the FIM (Vanbellingen *et al.*, 2016). A further advantage of the LIMOS is that it offers the possibility to separately assess the functional role of the upper limb in the ADLs ((Vanbellingen *et al.*, 2017); see Supplementary data for a detailed description)).

Continuous theta burst stimulation (cTBS) and sham protocol

cTBS was applied by means of a MagPro X100 stimulator (Medtronic Functional Diagnostics, Farum, Denmark), connected to a round coil with a 60mm outer radius (Magnetic Coil Transducer MC-125). The same cTBS protocol was used as previously described (Cazzoli *et al.*, 2009a; Cazzoli *et al.*, 2009b; Cazzoli *et al.*, 2012; Nyffeler *et al.*, 2008; Nyffeler *et al.*, 2009). In brief, the cTBS protocol comprised of 801 pulses, delivered in a continuous train of 267 bursts. Each burst consisted of 3 pulses at 30Hz, repeated at 6Hz. The duration of one single cTBS train was thus of 44 s. In order to test for a potential dose-response effect, the 30 neglect patients were randomly assigned to one out of three possible groups, i.e.: 8cTBS trains, 16cTBS trains, or sham stimulation. In the 8cTBS group, eight cTBS trains were applied over 2 days. Four cTBS trains were applied on Day 1 (two cTBS trains with an interval of 15 min, the third and the fourth cTBS train 60 and 75 min after the first one, respectively; see (Cazzoli *et al.*, 2012)), and four cTBS trains on Day 2 (same time intervals as for Day 1, repeated after 24 h). In the 16cTBS group, the same daily protocol was repeated four times, i.e., 16cTBS trains were applied over four days. Stimulation was applied over P3 (Cazzoli *et al.*, 2012; Nyffeler *et al.*, 2009), according to the international 10–20 EEG system, overlying the left PPC in proximity of the intraparietal sulcus (Hilgetag *et al.*, 2001). The coil was held tangentially to the scalp, with the handle pointing posteriorly, the current flowing clockwise as viewed from above. The patients were asked to close their eyes during stimulation application. cTBS was delivered at 100% of the patients' individual resting motor threshold. Sham stimulation was applied with the same 8cTBS protocol as described above, except for the use of a sham coil (Magnetic Coil Transducer MC-P-B70).

Statistical analyses

Baseline demographics (age, gender, years of education, handedness) and clinical characteristics (MoCA score, time after stroke onset in days, lesion volume in cm^3, lesion load of the

corticospinal tract (CST) in %, Jamar, stereognosis, NIHSS, CBS, FIM, LIMOS, and LIMOS upper limb scores) were compared across the three groups (sham, 8cTBS, 16cTBS) by means of separate, univariate analyses of variance (ANOVAs) for continuous variables, or by means of chi-squared tests for nominal variables.

The effects of cTBS between admission and discharge on neglect severity (ΔCBS T0-T1 and ΔComposite score T0-T1) and on functional outcome (ΔFIM T0-T1, ΔLIMOS T0-T1, ΔLIMOS upper limb T0-T1) were assessed by means of separate, univariate ANOVAs with the between-subjects factor group (sham, 8cTBS, 16cTBS).

To evaluate whether the effects of cTBS on neglect remained stable between discharge and follow-up three months later (ΔCBS T1-T2 and ΔComposite score T1-T2), we performed separate, univariate ANOVAs with the between-subjects factor group. The differences between time points (i.e., T0-T1 and T1-T2) were analysed separately because of the drop-out of some patients at T2 (a repeated-measures analysis approach would have caused the exclusion of these patients at all time points). For all analyses, post-hoc testing was performed by means of Fisher's least significant difference (LSD)-corrected t-tests.

Pearson's correlations were computed to explore how demographics (age, gender, years of education) and clinical characteristics (lesion volume, CST lesion load, length of stay, time post stroke, NIHSS and MoCA scores; additionally for neglect recovery and general functional outcome: Jamar and NSA scores) would relate to the cTBS effects, i.e., neglect recovery (ΔCBS) and general functional outcome (ΔFIM; ΔLIMOS; ΔLIMOS upper limb). Follow-up stepwise hierarchical regression analyses were applied where appropriate.

Hierarchical clustering analyses (according to the procedure outlined by (Winters *et al.*, 2017)), restricting the model to a maximum of two clusters, and using the nearest Euclidean distances method, were computed for two purposes. First, we investigated which patients would fit the predictions of the Proportional recovery rule (i.e., predicted recovery of ≈70% of the initial impairment within three months after stroke); henceforth referred to as rule-fitters and rule-non-

fitters. The proportional recovery rule is usually assessed at three months after stroke; we identified the number of patients belonging to the cluster of rule-fitters or rule-non-fitters within a time window shorter than three months, in order to assess whether cTBS could accelerate recovery concerning neglect severity (CBS) and general functional outcome (FIM, LIMOS, LIMOS upper limb). In order to evaluate whether cTBS would be able to reduce the detrimental effects of neglect on recovery, neglect severity and functional outcome parameters of rule-fitters and rule-non-fitters were then compared to the ones of the control group of RHS patients without neglect. Second, we assessed which patients would belong to the cluster of cTBS responders or non-responders, on the basis of their ΔCBS (T0-T1). This grouping was then used to identify the determinants of the variability of the cTBS effects in terms of lesion localisation, i.e., contrasting the lesions of cTBS responders vs. non-responders by means of a VLSM approach (please see the corresponding section for details).

Finally, we applied the Maugeri predictive model (Scrutinio *et al.*, 2017) to the data of our patients; this model calculates the probability of achieving a motor FIM score at discharge of > 61 points (i.e., indicating good outcome), based on demographics (age, gender) and clinical parameters (time post stroke, presence of neglect, motor and cognitive FIM scores at rehabilitation admission). In this context, we aimed to assess whether neglect patients treated with cTBS would recover beyond the probabilistic predictions of this model.

Data availability

Individual patient data collected in this study will not be openly distributed to conform with data privacy statement signed by our patients. However, specific aspects of the anonymized raw data, will be shared upon request.

RESULTS

Clinical and demographic baseline values in neglect patients

There were no significant baseline differences between the three cTBS groups (sham, 8cTBS, 16cTBS), neither in demographic, nor in clinical characteristics. Mean baseline data and analysis results are presented in Table 1, lesion overlap maps in Figure 1.

Table 1

about here

Figure 1

about here

---

cTBS significantly improves neglect recovery on a group level

We found a significant effect of the factor group on the improvement from admission to discharge, both in terms of CBS score (ΔCBS, T0-T1; $F_{[2,27]}$=3.46, p=0.04, η_p^2=0.20) and of composite score (ΔComposite score, T0-T1; $F_{[2,27]}$=7.80, p=0.002, η_p^2=0.37). Post-hoc testing showed that, compared to sham stimulation, ΔCBS was significantly higher both after 8cTBS (p=0.04) and 16cTBS (p=0.02; Figure 2A). Similarly, ΔComposite score was significantly higher after 8cTBS (p=0.001) and after 16cTBS (p=0.02; Figure 2B) as compared to sham stimulation. Hence, both cTBS protocols significantly improved neglect recovery from admission to discharge, both in the ADLs and in neuropsychological testing.

At follow-up testing three months after discharge (T2), three patients dropped-out concerning the CBS assessment, and four patients concerning the composite score assessment (see consort diagram in Supplementary Methods). In the remaining patients, the effect of the factor group was not significant, i.e., neglect severity remained stable between discharge and follow-up in all

three groups (ΔCBS, T1-T2; ($F_{[2,24]}$=0.65, p=0.94, η_p^2=0.005; ΔComposite score, T1-T2; $F_{[2,23]}$= 0.758, p=0.48, η_p^2=0.062; see Supplementary Figure 1).

Figure 2

about here

---

cTBS significantly improves general functional outcome on a group level

We found a significant effect of the factor group on FIM (ΔFIM, T0-T1; $F_{[2,27]}$=3.48, p=0.045, η_p^2=0.21), LIMOS (ΔLIMOS, T0-T1; $F_{[2,27]}$=6.76, p=0.004, η_p^2=0.33), and LIMOS upper limb (ΔLIMOS upper limb; T0-T1; $F_{[2,27]}$=3.65, p=0.04, η_p^2=0.21) improvement from admission to discharge (Figure 2, panels C-E). Post-hoc tests revealed that, compared to sham stimulation, ΔFIM was significantly higher both after 8cTBS (p=0.04) and 16cTBS (p=0.02). Similarly, compared to sham stimulation, ΔLIMOS was significantly higher after 8cTBS (p=0.003) and 16cTBS (p=0.005). This shows that both cTBS protocols significantly improved general functional outcome. Regarding ΔLIMOS upper limb, a significantly higher improvement was found for 8cTBS (p=0.02) compared to sham stimulation, whereas only a trend was found for 16cTBS (p=0.058). cTBS and sham protocols were well tolerated by all patients, without any side effects. The patients did not report any particular sensation during or after the cTBS or sham application.

Clinical and demographic factors predicting general functional outcome in neglect patients

We aimed at identifying the demographic and clinical factors correlating with the amelioration in general functional outcome, as assessed by FIM, LIMOS, and LIMOS upper limb. We found that the better the neglect recovery (ΔCBS), the better the general functional outcome, as

reflected both in FIM (ΔFIM; r=0.43; p=0.02) and LIMOS (ΔLIMOS; r=0.45; p=0.01; see Table 2) scores. Furthermore, the better the neglect recovery (ΔCBS), the better patients used their affected limb in their daily activities (ΔLIMOS upper limb; r=0.43; p=0.02). In addition, we found that the younger the patients, the better the general functional outcome (ΔFIM; r=-0.41; p=0.03). Also, the higher the cognitive resources at admission (as reflected by MoCA scores), the better the general functional outcome (ΔLIMOS; r=0.42; p=0.03). No significant correlations were found for the other clinical or demographic factors (see Table 2).

Therefore, we included these factors in the subsequent stepwise hierarchical regression analyses. NIHSS and CST lesion load were also included, since both are well-known outcome predictors (Harvey, 2015; Kwakkel *et al.*, 2010; Kwakkel and Kollen, 2013; Radlinska *et al.*, 2010). Several significant models predicting ΔFIM, ΔLIMOS, and ΔLIMOS upper limb were identified (see Table 3). In all models, neglect recovery (ΔCBS) was always the strongest predictor of general functional outcome, even when taking into account age, MoCA, NIHSS, and CST lesion load as additional factors.

Table 2

about here

Table 3

about here

---

cTBS accelerates recovery

We compared the predictions of the Proportional recovery rule (Marchi *et al.*, 2017; Ramsey *et al.*, 2017; Winters *et al.*, 2017) with our data concerning neglect severity (CBS scores) by applying hierarchical clustering. The proportion of rule-fitters, i.e., patients that already fitted the predictions of the Proportional recovery rule before three months, was considerably higher after cTBS (60% in the 8cTBS group; 80% in the 16cTBS group) than after sham stimulation (30%; Fig. 3, panels A-C). This shows that cTBS accelerated recovery of neglect.

We also compared the predictions of the Proportional recovery rule with our data concerning general functional outcome. For FIM scores, the proportion of rule-fitters was higher after cTBS (70% in the 8cTBS group; 80% in the 16cTBS group) than after sham stimulation (40%; Fig. 3, panels D-F). Crucially, after cTBS the proportion of rule-fitters was close to the one of patients with right-hemispheric damage but no neglect (93%; Supplementary Figure 2). This shows that cTBS accelerated recovery of general functional outcome and, by bringing the recovery rate of neglect patients close to the one of patients without neglect, seemed to eliminate the detrimental effects of neglect.

The same analyses conducted on the LIMOS and the LIMOS upper limb scores showed that cTBS accelerated recovery also in these measures (Supplementary Figure 3).

Figure 3

about here

---

25 % of neglect patients receiving cTBS improved more than predicted by the Maugeri predictive model

Based on clinical data at admission, the Maugeri predictive model calculates the probability of achieving a motor-FIM score of > 61 points at discharge, which defines a good motor out-

come. We compared the observed motor-FIM scores of our patients at discharge with the predicted values, as computed by means of the Maugeri predictive model ((Scrutinio *et al.*, 2017); supplementary Table 1). In our control group of RHD patients without neglect, 97% of the patients (i.e., 29 out of 30) followed the predictions of the model; only one patient had a worse motor outcome at discharge than predicted.

In the group of neglect patients undergoing cTBS, 25% of the patients (i.e., 5 out of 20; the groups undergoing 8 and 16cTBS trains considered together) reached a better motor outcome at discharge than predicted by the model, whereas 75% followed the predictions of the model. In the sham stimulation group, 90% of the patients (i.e., 9 out of 10) followed the predictions of the model, whereas only one patient had a slightly better motor outcome at discharge than predicted. Hence, a higher percentage of neglect patients treated with cTBS ameliorated beyond the predictions of the Maugeri predictive model.

Factors determining the variability of cTBS effects

We aimed to identify demographic and clinical factors that would influence the cTBS effects in neglect patients. We found no significant correlations between ΔCBS (T0-T1) and age (r=-0.15; p=0.42), sex (r=-0.06; p=0.74), years of education (r=-0.2; p=0.93), lesion volume (r=0.03; p=0.87), CST lesion load (r=0.05; p=0.79), length of stay (r=0.31; p=0.10), time post stroke (r=-0.10; p=0.60), NIHSS scores (r=0.04; p=0.84), or MoCA scores (r=0.22;p=0.26).

Next, based on the ΔCBS values (T0-T1), we performed a hierarchical cluster analysis in all neglect patients who received cTBS (i.e., 8cTBS and 16cTBS considered together), in order to discriminate cTBS responders from cTBS non-responders. The analysis identified 14 patients as cTBS responders, and 6 patients as cTBS non-responders (Figure 4A).

Figure 4

about here

A further analysis showed that the initial severity of neglect (i.e., CBS scores at admission) significantly correlated with ΔCBS in the group of cTBS responders (r=0.91; p<0.0001; Figure 4B), but not in the group of cTBS non-responders (r=0.10; p=0.85; Figure 4C).

In addition, we directly compared the scores of the subgroups (responders, non-responders, sham). Concerning neglect recovery (ΔCBS, T0-T1; main effect of group: $F_{[2,\ 27]}$=7.381, p=0.004, η_p^2=0.376), cTBS responders scored significantly better than the sham group (p=0.001) and the non-responders (p=0.007; Figure 4D). Concerning general functional outcome, cTBS responders scored better in the FIM (ΔFIM, T0-T1; main effect of group: $F_{[2,27]}$=3.877, p=0.033, η_p^2=0.223) than the sham group (p=0.01, Figure 4E), and better in the LIMOS (ΔLIMOS, T0-T1; main effect of group: $F_{[2,27]}$=10.084, p=0.001, η_p^2=0.428) than the sham group (p<0.001) and the non-responders (p=0.043; Supplementary Figure 4A), as well as better in the LIMOS upper limb (ΔLIMOS upper limb, T0-T1; main effect of group: $F_{[2,27]}$=8.482, p=0.001, η_p^2=0.386) than the sham group (p= 0.001) and the non-responders (p =0.008; Supplementary Figure 4B).

Finally, regarding the proportional recovery rule for neglect and general functional outcome (Figure 4F), a higher proportion of rule-fitters was observed in the cTBS responder subgroup (CBS: 100%; FIM: 86%) than in the sham group (CBS: 30%; FIM: 40%) and in the cTBS non-responder subgroup (CBS: 0%; FIM: 50%). Moreover, for the general functional outcome (FIM), the proportion of rule-fitters in the cTBS responder subgroup (86%) became similar to the one of the control group of RHD patients without neglect (93%).

In order to ascertain whether the location of the lesions of these two subgroups of neglect patients (i.e., cTBS non-responders and responders) would critically differ, we applied a VLSM approach. This analysis revealed a cluster of voxels that were significantly more often lesioned in cTBS non-responders than in cTBS responders (volume: 60 voxels). The probabilistic analysis

confirmed that the cluster was located in the right, posterior part of the corpus callosum (probability: 100%; MNI coordinates of the centre of mass of the cluster: 31, -39, 21; see Figure 5 and Supplementary Figure 5).

Interestingly, the cluster identified by our VLSM analysis lies in close proximity to a region of the posterior corpus callosum that has been deemed as critical for neglect severity, and which connects both posterior parietal cortices, as assessed by diffusion imaging and tract-based spatial statistics ((Bozzali *et al.*, 2012); see supplementary Figure 4). In addition, our cluster also lies close to a region of transcallosal projections of the posterior parietal cortices, whose anisotropy was significantly associated with interhemispheric inhibition processes induced by TMS applied over these cortical areas in healthy subjects ((Koch *et al.*, 2011); see supplementary Figure 5).

Figure 5

about here

DISCUSSION

Previous studies have shown that inhibitory NIBS of the left, intact hemisphere can trigger a significant amelioration of spatial neglect in patients with a right-hemispheric lesion (Brighina *et al.*, 2003; Cazzoli *et al.*, 2012; Koch *et al.*, 2012; Nyffeler *et al.*, 2009; Salazar *et al.*, 2018; Sparing *et al.*, 2009). However, the effects of this stimulation present with a considerable inter-individual variability (Lefaucheur *et al.*, 2014), which is scarcely understood. According to recent findings (Umarova *et al.*, 2016), the role of the contralesional hemisphere in neglect could be compensatory, rendering its inhibitory stimulation even detrimental. Moreover, recent accounts postulate that the recovery of stroke in general, and of neglect in particular, would follow

fixed patterns, which are not susceptible of being influenced by therapeutic approaches (Marchi *et al.*, 2017; Ramsey *et al.*, 2017; Stinear *et al.*, 2017; Winters *et al.*, 2017). The aim of the present randomized, double-blind, sham controlled study was thus to address these open, controversial issues. More specifically, we aimed to clarify which neglect patients, and through which determinants and mechanisms, would benefit from inhibitory, non-invasive brain stimulation of the left, intact hemisphere. For this purpose, we applied inhibitory cTBS, and comprehensively assessed the characteristics and the determinants of its effects on spatial neglect, i.e.: a possible dose-response relationship, the magnitude and length of the effects and, most importantly, inter-individual differences in responsiveness. Finally, we aimed to assess how spatial neglect, and its possible amelioration through cTBS, would influence general functional outcome, as measured with the FIM and the LIMOS, and affect recovery dynamics as predicted by the Proportional recovery rule and the Maugeri predictive model.

On a group level, both cTBS protocols (i.e., 8 and 16cTBS trains) triggered a significant and a long-lasting improvement of neglect and of general functional outcome. However, at the individual level, an important variability of these effects was observed. We will first comment on the effects at the group level, and then discuss the identified factors that contribute to their inter-individual variability.

The rationale for applying inhibitory NIBS over the left, intact PPC is provided by the presence of a pathological hyper-excitability within this area (Corbetta *et al.*, 2005; Koch *et al.*, 2008; Paladini *et al.*, 2017), which is due to maladaptive interhemispheric inhibition mechanisms (in animals, e.g., (Palmer *et al.*, 2012; Payne and Rushmore, 2004; Rushmore *et al.*, 2006; Sprague, 1966; Valero-Cabre *et al.*, 2006); in humans, e.g., (Corbetta *et al.*, 2005; He *et al.*, 2007; Koch *et al.*, 2008; Vuilleumier *et al.*, 1996). A reduction of this hyper-excitability using cTBS, with a subsequent improvement of neglect, has been shown to last up to 3-4 weeks (Cazzoli *et al.*, 2012; Koch *et al.*, 2012). Building on findings in animal models concerning LTP/LTD-like phenomena associated with late-phase synaptic plasticity mechanisms (Woo and

Nguyen, 2003; Zhou *et al.*, 2003), several studies in humans have shown that the number of applied trains is an influential factor in determining the duration of the cTBS effects (Goldsworthy *et al.*, 2012; Nyffeler *et al.*, 2006; Nyffeler *et al.*, 2009). In particular, the repeated, spaced cTBS application seems able to "stabilize and lock" the excitability within the stimulated area (Cazzoli *et al.*, 2015; Goldsworthy *et al.*, 2015). In the present study, both 8 and 16cTBS trains similarly improved neglect for a period of up to six weeks, both at the level of the ADLs and of neuropsychological testing. There is therefore no clear evidence for an advantage, in terms of amplitude or duration of the effects, in administering more than 8cTBS trains, at least when these are combined with smooth pursuit training. This suggests that, after 8cTBS trains, the over-excitability of the left, intact PPC may have already been reduced at a sufficiently low level, and may be resistant to reversal by physiological activity, due to consolidated synaptic plasticity (Goldsworthy *et al.*, 2015). In the follow-up measurement at 3 months after discharge, the observed neglect recovery remained stable. This is also in keeping with the results of previous studies, showing that neglect recovery is strongest during the early post-stroke phase (Buxbaum *et al.*, 2004; Ramsey *et al.*, 2016).

Recent studies showed that the recovery of neglect follows the predictions of the Proportional recovery rule, i.e., patients recover from ≈70% of their initial impairment within 3 months after stroke, irrespectively of therapy dose (Marchi *et al.*, 2017; Ramsey *et al.*, 2017; Winters *et al.*, 2017). In the present study, we showed that, well before a period of three months, a considerable proportion of patients who underwent cTBS (i.e., 80% after 16cTBS and 60% after 8cTBS trains) were already rule-fitters, i.e., fitted the predictions of the Proportional recovery rule. In contrast, only 30% of patients in the sham group were rule-fitters. This clearly demonstrates that cTBS accelerates the recovery of neglect. To the best of our knowledge, this is the first study to demonstrate that a therapeutic intervention can positively influence the natural stroke recovery dynamics predicted by the Proportional recovery rule.

At the individual level, hierarchical cluster analysis allowed us to distinguish between cTBS responders (who showed a significantly better neglect recovery than the one following sham stimulation) and non-responders (who showed a neglect recovery equal to the one following sham stimulation). In cTBS responders, the initial neglect severity significantly correlated with its recovery, whereas this was not the case in non-responders. This finding is in line with the fact that the higher the over-excitability of the left, intact PPC (and the more severe the neglect symptoms), the stronger the neglect amelioration induced by TMS application (Koch *et al.*, 2008). Moreover, all patients classified as rule-fitters according to the Proportional recovery rule belonged to the cTBS responder subgroup, strengthening the convergent validity of these categorizations.

Several clinical and demographic parameters (i.e., age, sex, MoCA score, years of education, handedness, time after stroke, length of stay, lesion volume, and initial NIHSS score) were not able to predict whether patients would respond to cTBS or not. However, VLSM and probabilistic white matter fibre tract disconnection analyses revealed that, unlike responders, cTBS non-responders presented with a lesion involving the posterior part of the corpus callosum. Interestingly, the location of this lesion cluster lies within the transcallosal inhibitory projections interconnecting the two homologous superior parietal lobules (Koch *et al.*, 2011). Damage to these transcallosal projections was found to be associated with the severity (Bozzali *et al.*, 2012) and the persistence (Lunven *et al.*, 2015) of neglect. In line with these findings, the structural variability within the corpus callosum in healthy individuals, consistent with differential effects on inter-hemispheric interactions, was able to predict the individual differences in the effects of PPC cTBS on the spatial allocation of attention (Chechlacz *et al.*, 2015).

Moreover, a breakdown of functional connectivity between the attentional networks of the two hemispheres has been identified as a crucial mechanism leading to neglect, with a loss of inter-hemispheric correlations between activity patterns, and a relative imbalance in task-evoked activity (Baldassarre *et al.*, 2014; Carter *et al.*, 2010; He *et al.*, 2007). Accordingly, the recovery

of neglect is significantly correlated with an improvement in the initially depressed inter-hemispheric functional connectivity between PPCs (Ramsey *et al.*, 2016). Our results corroborate these findings, showing that cTBS can contribute to neglect recovery when the transcallosal connectivity of the two PPCs (Corbetta and Shulman, 2011) is intact. cTBS has also been shown to enhance functional connectivity between the stimulated area and other, remote but interconnected, cortical areas (Cao *et al.*, 2016). This suggests that, in responding neglect patients, cTBS can not only reduce the over-excitability of the left, intact PPC (Koch *et al.*, 2008), but may also improve the initially depressed inter-hemispheric functional connectivity between PPCs. This may thus functionally 'reintegrate' the left PPC into the attentional networks, i.e., re-instate its functional role in attentional processes.

This view is also consistent with growing evidence that recovery of post-stroke deficits such as neglect depends, at least in part, on the non-damaged hemisphere (see, e.g., Bartolomeo *et al.*, 2007; Lunven *et al.*, 2015; Umarova *et al.*, 2016; see also Bartolomeo & Thiebaut de Schotten, 2016 for a recent review). In fact, the pathological hyper-excitability of the left, contralesional PPC can be interpreted as a loss of functional connectivity of this area, as illustrated above. In turn, the functional connectivity of this area may ameliorate when its pathological hyperexcitability is reduced by means of inhibitory non-invasive brain stimulation. This may be the primary mechanism of the cTBS-induced neglect recovery, and could also explain why, in our study, an inhibition of the contralesional PPC with cTBS did not result in a worsening of neglect symptoms in any patient or outcome measure.

Another factor potentially influencing the functional role of the left, intact PPC in neglect remission may be the specific post-stroke phase. Whereas all patients in the study by Umarova and colleagues (Umarova *et al.*, 2016) were tested in the acute phase (i.e., <10 days post-stroke), patients in the present study were in the subacute phase (i.e., 24 days post-stroke on average). Nevertheless, our regression analyses showed that the post-stroke time interval was not a predictive factor for the positive cTBS effects.

As mentioned above, cTBS also significantly ameliorated general functional outcome, as measured by standardized measures, such as the FIM (Keith *et al.*, 1987) and the recently developed LIMOS (Ottiger *et al.*, 2015; Vanbellingen *et al.*, 2016). To account for the contribution of demographic and clinical factors to general functional outcome, we first identified several of these factors in separate multiple regression analyses. Neglect recovery, age, and MoCA were identified as significant predictors of general functional outcome, in keeping with the findings of previous studies (Bagg *et al.*, 2002; Nijboer *et al.*, 2013; Nijboer *et al.*, 2014; Vanbellingen *et al.*, 2017). In the subsequent analyses, we therefore included these factors, along with NIHSS (Harvey, 2015; Kwakkel *et al.*, 2010; Kwakkel and Kollen, 2013) and CST lesion load (Radlinska *et al.*, 2010). Neglect recovery was the strongest predictor of general functional outcome, even taking into account age, MoCA, NIHSS, and CST lesion load as additional factors. In fact, the amplitude of the cTBS-induced neglect improvement was significantly associated with better ADL performance. Moreover, hierarchical cluster analyses showed that the improvement of general functional outcome was significantly larger in cTBS responders than in non-responders. Analyses applying the Proportional recovery rule (Stinear *et al.*, 2017) also showed that cTBS, by ameliorating neglect, accelerated general functional outcome, as measured with the FIM and LIMOS. More importantly, a comparison of the cTBS responder subgroup with our control sample further showed that the application of cTBS brought the level of functional recovery of patients with neglect close to the one of patients with right-hemispheric damage but no neglect. This suggests that cTBS can substantially reduce the detrimental effects of neglect on stroke recovery. These findings are further supported by analyses based on the Maugeri predictive model, in which neglect is integrated as a crucial predictor of outcome after stroke (Scrutinio *et al.*, 2017). We applied this model to the data of each single patient of our sample, which matched well, in terms of time post stroke and length of stay, the large retrospective sample of the study by Scrutinio and colleagues (Scrutinio *et al.*, 2017). Our results showed that 25% of the neglect patients who underwent cTBS had a better outcome than the one predict-

ed by the model. For the other patients, the outcome accurately followed the predictions of the model, therefore confirming a high external validity of the latter.

Similarly to the general ADL improvement, we also found a significant association between LIMOS upper limb scores, which describe upper limb use in the ADL, and neglect outcome. Beside CST lesion load, which is a well-known outcome predictor (Stinear *et al.*, 2012), our analyses showed that neglect recovery was also a strong predictor of upper limb use. These results confirm the recent findings showing that neglect is an important, independent factor affecting upper limb use in the ADL (Vanbellingen *et al.*, 2017). In addition, the amount of recovery of upper limb function in everyday life (as measured with the LIMOS upper limb) was increased after cTBS, in particular in the cTBS responder subgroup, and the dynamics of its recovery were positively influenced.

It is to note that all our neglect patients received, additionally to best-practice inpatient rehabilitative therapies, also smooth pursuit training (SPT). SPT is known to facilitate multimodal attentional shifts towards the neglected side of space, and to improve neglect on the ADL level (Kerkhoff *et al.*, 2014; Mattingly *et al.*, 1994). Previous studies have shown that combined neglect therapies have superior effects than single ones (Schindler *et al.*, 2002; Schroder *et al.*, 2008). In the present study, we chose to administer both cTBS and SPT because this combination has recently been shown to significantly enhance treatment effects (Hopfner *et al.*, 2015).

The limitations of our study include the fact that we did not test our patients in strictly defined time intervals, as it has been done in prospective prognostic neglect studies (Marchi *et al.*, 2017; Winters *et al.*, 2017). Nevertheless, all patients in our study followed a similar hospitalisation course, and the results presented were obtained in a completely data-driven fashion. Furthermore, the not strictly defined assessment time intervals allowed us to analyse whether post-stroke time or length of stay would represent predictive factors for the cTBS effects. Another limitation of our study is that lesion analysis was based only on high resolution, three dimensional MRI scans. In future studies, additional diffusion imaging, with tract-based spatial statis-

tics, possibly using neuronavigation and focal stimulation in order to target narrower cortical areas, would be a promising approach to explore the role of intra- and interhemispheric connections in further detail. Finally, the sample of our study was relatively small. Larger multi-centre studies are needed to better characterize the therapeutic effects of cTBS after stroke and to more comprehensively stratify patients.

Nevertheless, the present study sheds more light on the mechanisms and determinants of NIBS. It demonstrates for the first time that in subacute right hemispheric stroke patients who present an intact corpus callosum, general functional outcome can be substantially improved and accelerated when neglect recovery is ameliorated by the inhibition of the left, intact PPC by means of cTBS. This suggests that cTBS improves inter-hemispheric parieto-parietal connectivity, thereby rebalancing activity patterns across the nodes of the attentional networks of the two hemispheres.

ACKNOWLEDGMENTS AND FUNDING

This study was supported by grants of the Swiss National Science Foundation (T.N. 320030_140696 and 320030_169789; D.C. PZ00P3_154714/1) and Birmingham-Illinois Partnership for Discovery, Engagement and Education (BRIDGE) Fellowship (M.C.).

DISCLOSURES OR CONFLICTS OF INTEREST

None.

FIGURE LEGENDS

Figure 1- Lesion overlap maps of the 30 patients in the three stimulation conditions.

Lesion overlap maps of the 30 patients in the three stimulation conditions (sham stimulation, 8cTBS, 16cTBS). The color-coded legend indicates the number of patients with damage to a specific brain region. The lesion overlap maps are plotted on the CH2 template, as available in MRIcron (http://www.mccauslandcenter.sc.edu/crnl/chris-rordens-neuropsychology-lab). Axial slices are oriented according to the neurological convention. The z-position of each axial slice, in MNI coordinates, is indicated by the numbers at the top of the figure, and also depicted by the blue lines on the sagittal slice (top left of the figure).

Figure 2 – Improvement between admission and discharge from neurorehabiliation.

(A) CBS improvement between admission to and discharge from neurorehabilitation (T0-T1). **(B)** Improvement in the neglect composite score between admission to and discharge from neurorehabilitation (T0-T1). **(C, D, E)** Improvement of the functional outcome (FIM Total, LIMOS Total and, with particular reference to arm involvement, LIMOS Upper Limb) between admission to and discharge from neurorehabilitation. Results are shown as whisker plots; each box representing the upper to the lower quartiles with whiskers extending to the minimum and maximum of 1.5 times the interquartile range, Mean values per group are indicated by the blue line and individual data by grey points. Asterisks represent significant post-hoc tests between the three stimulation conditions (sham, 8cTBS, 16cTBS; ** $p < .01$, * $p < .05$).

Figure 3 – Expected versus measured scores for CBS and FIM according the Proportional recovery rule.

Expected CBS scores according the Proportional recovery rule (i.e., recovery of ≈70% of the initial impairment, irrespective of therapy; y-axis), and measured CBS scores at discharge, i.e. before 3 months (x-axis), separately presented for the three stimulation groups. Hierarchical

clustering revealed that only 30% of patients receiving sham stimulation fitted the predictions of the Proportional recovery rule at discharge **(A)**. In contrast, 60 % of neglect patients undergoing 8cTBS trains **(B)**, and 80% of neglect patients undergoing 16cTBS trains **(C)** already fitted the predictions of the Proportional recovery rule at discharge.

Expected FIM scores according the Proportional recovery rule (i.e., recovery of ≈70% of the initial impairment, irrespective of therapy; y-axis), and measured FIM scores at discharge (x-axis), separately presented for the three stimulation groups. Hierarchical clustering revealed that only 40% of neglect patients receiving sham stimulation fitted the predictions of the Proportional recovery rule **(D)**. In contrast, 70 % of the neglect patients already fitted these predictions in the 8cTBS group **(E)**, and 80% of the neglect patients in the 16cTBS condition **(F)**. The dotted lines represent perfect predictions of the Proportional recovery rule (i.e., score predicted by the rule perfectly corresponding to the score measured at discharge at 3 months).

Figure 4 – Comparing cTBS responders and cTBS non-responders.

A. CBS scores at admission, plotted against CBS scores at discharge, for all neglect patients who received cTBS (i.e., 8cTBS and 16cTBS considered together); the dotted line represents the absence of change. Based on a hierarchical cluster analysis, patients were divided into cTBS responders and cTBS non-responders. **B.** In the group of cTBS responders, the severity of neglect at admission significantly correlated with the cTBS effects (in terms of ΔCBS); **C.** this was not the case in the group of cTBS non-responders. In cTBS responders, neglect recovery (**D**) and general functional outcome (**E**) were significantly improved. **F.** A higher proportion of fitters (as defined with respect to the Proportional recovery rule) was observed in the cTBS responder subgroup than in the sham group and in the cTBS non-responder subgroup, both concerning neglect severity (CBS) and general functional outcome (FIM). Results in Subplot A, B and C are shown as scatter plots; individual values of responders and non-responders are indicated in black, and white respectively. The grey line represents the correlation of the variables plotted on the x and

y-axis. Results of subplots D and E shown as whisker plots; each box representing the upper to the lower quartiles with whiskers extending to the minimum and maximum of 1.5 times the interquartile range, Mean values per group are indicated by the blue line and individual data by grey points Asterisks represent significant post-hoc tests (*** p≤.001; ** p<.01).

Figure 5 - Lesion overlap maps and results of the VLSM analysis comparing cTBS responders and non-responders.

Lesion overlap maps in the subgroup of cTBS non-responders (**A**) and of cTBS responders (**B**). The colour-coded legend indicates the number of patients with damage to a specific brain region. **C.** Lesion subtraction plot (i.e., cTBS non-responders minus cTBS responders). The colour-coded legend indicates the difference percent overlap. The lesion overlap maps and the subtraction plot are represented on the CH2 template, as available in MRIcron (http://www.mccauslandcenter.sc.edu/crnl/chris-rordens-neuropsychology-lab). Axial slices are oriented according to the neurological convention. The z-position of each axial slice, in MNI coordinates, is indicated by the numbers at the top of the figure, and also depicted by the blue, horizontal lines on the sagittal slice (bottom right of the figure). **D.** Results of the VLSM analysis. Voxels that were significantly more often lesioned in cTBS non-responders are depicted in red (significance level $p < 0.05$, based on the Liebermeister test, FDR-corrected, 4000 permutations). The corpus callosum and its projections are depicted in yellow, according to published probabilistic diffusion tensor imaging (DTI) tractography atlases (Rojkova *et al.*, 2016; Thiebaut de Schotten *et al.*, 2011); the probability for voxels to belong to the corpus callosum is set at >50% (i.e., above chance). The lesion cluster and the corpus callosum are displayed on the CH2 template, as available in MRIcron (http://www.mccauslandcenter.sc.edu/crnl/chris-rordens-neuropsychology-lab). The axial and coronal slices are oriented according to the neurological convention. The z-position of each axial and the y-position of each coronal slice, in MNI coordinates, is indicated by the numbers at the top of each slice, and is also depicted by the blue, hori-

zontal lines on the sagittal slice (for axial slices) and by the blue, vertical lines on the sagittal slice (for coronal slices) at the bottom right of the figure. The significant lesion cluster (60 voxels) is located in the right, posterior part of the corpus callosum (MNI coordinates of the centre of mass of the cluster: 31, -39, 21).

REFERENCES

Azouvi P, Samuel C, Louis-Dreyfus A, Bernati T, Bartolomeo P, Beis JM, et al. Sensitivity of clinical and behavioural tests of spatial neglect after right hemisphere stroke. J Neurol Neurosurg Psychiatry 2002; 73; 160-6.

Azouvi P. The ecological assessment of unilateral neglect. Ann Phys Rehabil Med 2017; 60; 186-190.

Bagg S, Pombo AP, Hopman W. Effect of age on functional outcomes after stroke rehabilitation. Stroke 2002; 33; 179-85.

Baldassarre A, Ramsey L, Hacker CL, Callejas A, Astafiev SV, Metcalf NV, et al. Large-scale changes in network interactions as a physiological signature of spatial neglect. Brain 2014; 137; 3267–3283.

Bartolomeo P, Thiebaut de Schotten M, Doricchi F. Left unilateral neglect as a disconnection syndrome. Cereb Cortex 2007; 17; 2479-90.

Bartolomeo P., Thiebaut de Schotten M. Let thy left brain know what thy right brain doeth: Inter-hemispheric compensation of functional deficits after brain damage. Neuropsychologia 2016; 93; 407–412.

Becker BJ. Synthesizing standardized mean-change measures. Br J Math Stat Psychol 1988; 41 257–78.

Bozzali M, Mastropasqua C, Cercignani M, Giulietti G, Bonni S, Caltagirone C, et al. Microstructural damage of the posterior corpus callosum contributes to the clinical severity of neglect. PLoS One 2012; 7; e48079.

Brighina F, Bisiach E, Oliveri M, Piazza A, La Bua V, Daniele O, et al. 1 Hz repetitive transcranial magnetic stimulation of the unaffected hemisphere ameliorates contralesional visuospatial neglect in humans. Neurosci Lett 2003; 336; 131-3.

Brunila T, Jalas M, Lindell JA, Tenovuo O, Hamalainen H. The two part picture in detection of visuospatial neglect. Clin Neuropsychol 2003; 17; 45-53.

Buxbaum LJ, Ferraro MK, Veramonti T, Farne A, Whyte J, Ladavas E, et al. Hemispatial neglect Subtypes, neuroanatomy, and disability. NEUROLOGY 2004; 62; 749–756.

Cao L, Fu W, Zhang Y, Huo S, Du J, Zhu L, et al. Intermittent theta burst stimulation modulates resting-state functional connectivity in the attention network and promotes behavioral recovery in patients with visual spatial neglect. Neuroreport 2016; 27; 1261-1265.

Carter AR, Astafiev SV, Lang CE, Connor LT, Rengachary J, Strube MJ, et al. Resting interhemispheric functional magnetic resonance imaging connectivity predicts performance after stroke Annals of Neurology 2010; 67; 365-375.

Cazzoli D, Muri RM, Hess CW, Nyffeler T. Horizontal and vertical dimensions of visual extinction: a theta burst stimulation study. Neuroscience 2009a; 164; 1609-14.

Cazzoli D, Wurtz P, Muri RM, Hess CW, Nyffeler T. Interhemispheric balance of overt attention: a theta burst stimulation study. Eur J Neurosci 2009b; 29; 1271-6.

Cazzoli D, Müri R, Schumacher R, von Arx S, Chaves S, Gutbrod K, et al. Theta burst stimulation reduces disability during the activities of daily living in spatial neglect. Brain 2012; 135; 3426-39.

Cazzoli D, Rosenthal CR, Kennard C, Zito GA, Hopfner S, Muri RM, et al. Theta burst stimulation improves overt visual search in spatial neglect independently of attentional load. Cortex 2015; 73; 317-29.

Cazzoli D, Hopfner S, Preisig B, Zito G, Vanbellingen T, Jager M, et al. The influence of naturalistic, directionally non-specific motion on the spatial deployment of visual attention in right-hemispheric stroke. Neuropsychologia 2016; 92; 181-189.

Chechlacz M, Humphreys GW, Sotiropoulos SN, Kennard C, Cazzoli D. Structural Organization of the Corpus Callosum Predicts Attentional Shifts after Continuous Theta Burst Stimulation. J Neurosci 2015; 35; 15353-68.

Chen HM, Chen CC, Hsueh IP, Huang SL, Hsieh CL. Test-retest reproducibility and smallest real difference of 5 hand function tests in patients with stroke. Neurorehabil Neural Repair 2009; 23; 435-40.

Chiti G, Pantoni L. Use of Montreal Cognitive Assessment in patients with stroke. Stroke 2014; 45; 3135-40.

Cocchini G, Beschin N, Jehkonen M. The fluff test: a simple task to assess body representational neglect. Neuropsychological Rehabilitation 2001; 11; 17-31.

Corbetta M, Kincade MJ, Lewis C, Snyder AZ, Sapir A. Neural basis and recovery of spatial attention deficits in spatial neglect. Nat Neurosci 2005; 8; 1603-10.

Corbetta M, Shulman GL. Spatial Neglect and Attention Networks. Annu Rev Neurosci 2011; 34; 569-599.

Gauthier L, Dehaut F, Joanette Y. The Bells test: A quantitative and qualitative test for visual neglect. International Journal of Clinical Neuropsychology 1989; 11; 49-54.

Goldsworthy MR, Pitcher JB, Ridding MC. The application of spaced theta burst protocols induces long-lasting neuroplastic changes in the human motor cortex. Eur J Neurosci 2012; 35; 125-34.

Goldsworthy MR, Muller-Dahlhaus F, Ridding MC, Ziemann U. Resistant Against De-depression: LTD-Like Plasticity in the Human Motor Cortex Induced by Spaced cTBS. Cereb Cortex 2015; 25; 1724-34.

Grawe K, Braun U. Qualitätskontrolle in der Psychotherapiepraxis. Zeitschrift für klinische Psychologie 1994; 23; 242–67.

Harvey RL. Predictors of Functional Outcome Following Stroke. Phys Med Rehabil Clin N Am 2015; 26; 583-98.

He BJ, Snyder AZ, Vincent JL, Epstein A, Shulman GL, Corbetta M. Breakdown of functional connectivity in frontoparietal networks underlies behavioral deficits in spatial neglect. Neuron 2007; 53; 905-18.

Hilgetag CC, Theoret H, Pascual-Leone A. Enhanced visual spatial attention ipsilateral to rTMS-induced 'virtual lesions' of human parietal cortex. Nat Neurosci 2001; 4; 953-7.

Hopfner S, Cazzoli D, Müri RM, Nef T, Mosimann UP, Bolhlhalter S, et al. Enhancing treatment effects by combining continuous theta burst stimulation with smooth pursuit training. neuropschologia 2015; 74; 145-51.

Huang YZ, Edwards MJ, Rounis E, Bhatia KP, Rothwell JC. Theta burst stimulation of the human motor cortex. Neuron 2005; 45; 201-6.

Kaufmann BC, Frey J, Pflugshaupt T, Wyss P, Paladini RE, Vanbellingen T, et al. The spatial distribution of perseverations in neglect patients during a nonverbal fluency task depends on the integrity of the right putamen. Neuropsychologia 2018;

Keith RA, Granger CV, Hamilton BB, Sherwin FS. The functional independence measure: a new tool for rehabilitation. Adv Clin Rehabil 1987; 1; 6-18.

Kerkhoff G, Bucher L, Brasse M, Leonhart E, Holzgraefe M, Volzke V, et al. Smooth Pursuit "Bedside" Training Reduces Disability and Unawareness During the Activities of Daily Living in Neglect: A Randomized Controlled Trial. Neurorehabil Neural Repair 2014; 28; 554-63.

Kinsbourne M, 1987. Mechanisms of unilateral Neglect. In: Neurophysiological and Neuropsychological Aspects of Spatial neglect. Vol., M. Jeannerod, Elsevier Science, pp. 69-86.

Koch G, Oliveri M, Cheeran B, Ruge D, Lo Gerfo E, Salerno S, et al. Hyperexcitability of parietal-motor functional connections in the intact left-hemisphere of patients with neglect. Brain 2008; 131; 3147-55.

Koch G, Cercignani M, Bonni S, Giacobbe V, Bucchi G, Versace V, et al. Asymmetry of parietal interhemispheric connections in humans. J Neurosci 2011; 31; 8967-75.

Koch G, Bonni S, Giacobbe V, Bucchi G, Basile B, Lupo F, et al. theta-burst stimulation of the left hemisphere accelerates recovery of hemispatial neglect. Neurology 2012; 78; 24-30.

Kwakkel G, Veerbeek JM, E.E. vW, Nijland R, Harmeling-van der Wel BC, Dippel DWJ. Predictive value of the NIHSS for ADL outcome after ischemic hemispheric stroke: does timing of early assessment matter? J Neurol Sci 2010;

Kwakkel G, Kollen BJ. Predicting activities after stroke: what is clinically relevant? Int J Stroke 2013; 8; 25-32.

Lefaucheur J, Andre-Obadia N, Antal A, Ayache S, Baeken C, Benninger D, et al. Evidence-based guidelines on the therapeutic use of repetitive transcranial magnetic stimulation (rTMS). Clinical Neurophysiology 2014; 125; 2150-2206.

Lincoln N, Jackson J, Adams S. Reliability and revision of the Nottingham sensory assessment for stroke patients. Physiotherapy 1998;

Lundervold AJ, Bergmann N, Wootton C. Visual neglect in the first weeks after a stroke in the right hemisphere. Scand J Psychol 2005; 46; 297-303.

Lunven M, Thiebaut De Schotten M, Bourlon C, Duret C, Migliaccio R, Rode G, et al. White matter lesional predictors of chronic visual neglect: a longitudinal study. Brain 2015; 138; 746-60.

Marchi NA, Ptak R, Di Pietro M, Schnider A, Guggisberg AG. Principles of proportional recovery after stroke generalize to neglect and aphasia. Eur J Neurol 2017; 24; 1084-1087.

Mattingly RR, Sorisky A, Brann MR, Macara IG. Muscarinic receptors transform NIH 3T3 cells through a Ras-dependent signalling pathway inhibited by the Ras-GTPase-activating protein SH3 domain. Mol Cell Biol 1994; 14; 7943-52.

Nijboer T, van de Port I, Schepers V, Post M, Visser-Meily A. Predicting functional outcome after stroke: the influence of neglect on basic activities in daily living. Front Hum Neurosci 2013; 7; 182.

Nijboer TC, Kollen BJ, Kwakkel G. The impact of recovery of visuo-spatial neglect on motor recovery of the upper paretic limb after stroke. PLoS One 2014; 9; e100584.

Nyffeler T, Wurtz P, Luscher HR, Hess CW, Senn W, Pflugshaupt T, et al. Extending lifetime of plastic changes in the human brain. Eur J Neurosci 2006; 24; 2961-6.

Nyffeler T, Cazzoli D, Wurtz P, Luthi M, von Wartburg R, Chaves S, et al. Neglect-like visual exploration behaviour after theta burst transcranial magnetic stimulation of the right posterior parietal cortex. Eur J Neurosci 2008; 27; 1809-13.

Nyffeler T, Cazzoli D, Hess C, Müri R. One session of repeated parietal theta burst stimulation trains induces long-lasting im-provement of visual neglect. Stroke. Stroke 2009; 40; 2791-2796.

Ottiger B, Vanbellingen T, Gabriel C, Huberle E, Koenig-Bruhin M, Pflugshaupt T, et al. Correction: Validation of the New Lucerne ICF Based Multidisciplinary Observation Scale (LIMOS) for Stroke Patients. PLoS One 2015; 10; e0134186.

Paladini RE, Muri RM, Meichtry J, Nef T, Mast FW, Mosimann UP, et al. The Influence of Alertness on the Spatial Deployment of Visual Attention is Mediated by the Excitability of the Posterior Parietal Cortices. Cereb Cortex 2017; 27; 233-243.

Palmer LM, Schulz JM, Murphy SC, Ledergerber D, Murayama M, Larkum ME. The cellular basis of GABA(B)-mediated interhemispheric inhibition. Science 2012; 335; 989-93.

Payne BR, Rushmore RJ. Functional circuitry underlying natural and interventional cancellation of visual neglect. Exp Brain Res 2004; 154; 127-53.

Radlinska B, Ghinani S, Leppert IR, Minuk J, Pike GB, Thiel A. Diffusion tensor imaging, permanent pyramidal tract damage, and outcome in subcortical stroke. Neurology 2010; 75; 1048-54.

Ramsey LE, Siegel JS, Baldassarre A, Metcalf NV, Zinn K, Shulman GL, et al. Normalization of network connectivity in hemispatial neglect recovery. Ann Neurol 2016; 80; 127-41.

Ramsey LE, Siegel JS, Lang CE, Strube M, Shulman GL, Corbetta M. Behavioural clusters and predictors of performance during recovery from stroke. Nat Hum Behav 2017; 1;

Ringman JM, Saver JL, Woolson RF, Clarke WR, Adams HP. Frequency, risk factors, anatomy, and course of unilateral neglect in an acute stroke cohort. Neurology 2004; 63; 468-74.

Rojkova K, Volle E, Urbanski M, Humbert F, Dell'Acqua F, Thiebaut de Schotten M. Atlasing the frontal lobe connections and their variability due to age and education: a spherical deconvolution tractography study. Brain Structure and Function 2016; 221; 1751-1766.

Rorden C, Karnath HO. A simple measure of neglect severity. Neuropsychologia 2010; 48; 2758-2763.

Rossi S, Hallett M, Rossini PM, Pascual-Leone A. Safety, ethical considerations, and application guidelines for the use of transcranial magnetic stimulation in clinical practice and research. Clinical Neurophysiology 2009; 120; 2008-2039.

Rushmore RJ, Valero-Cabre A, Lomber SG, Hilgetag CC, Payne BR. Functional circuitry underlying visual neglect. Brain 2006; 129; 1803-21.

Salazar APS, Vaz PG, Marchese RR, Stein C, Pinto C, Pagnussat AS. Noninvasive Brain Stimulation Improves Hemispatial Neglect After Stroke: A Systematic Review and Meta-Analysis. Arch Phys Med Rehabil 2018; 99; 355-366 e1.

Schenkenberg T, Bradford DC, Ajax ET. Line bisection and unilateral visual neglect in patients with neurologic impairment. Neurology 1980; 30: 509-17.

Schindler I, Kerkhoff G, Karnath HO, Keller I, Goldenberg G. Neck muscle vibration induces lasting recovery in spatial neglect. J Neurol Neurosurg Psychiatry 2002; 73; 412-9.

Schroder A, Wist ER, Homberg V. TENS and optokinetic stimulation in neglect therapy after cerebrovascular accident: a randomized controlled study. Eur J Neurol 2008; 15; 922-7.

Scrutinio D, Lanzillo B, Guida P, Mastropasqua F, Monitillo V, Pusineri M, et al. Development and Validation of a Predictive Model for Functional Outcome After Stroke Rehabilitation: The Maugeri Model. Stroke 2017; 48; 3308-3315.

Sparing R, Thimm M, Hesse MD, Kust J, Karbe H, Fink GR. Bidirectional alterations of interhemispheric parietal balance by non-invasive cortical stimulation. Brain 2009; 132; 3011-20.

Sprague JM. Interaction of cortex and superior colliculus in mediation of visually guided behavior in the cat. Science 1966; 153; 1544-7.

Stinear CM, Barber PA, Petoe M, Anwar S, Byblow WD. The PREP algorithm predicts potential for upper limb recovery after stroke. Brain 2012; 135; 2527-35.

Stinear CM, Byblow WD, Ackerley SJ, Smith MC, Borges VM, Barber PA. Proportional Motor Recovery After Stroke: Implications for Trial Design. Stroke 2017; 48; 795-798.

Thiebaut de Schotten M, Ffytche DH, Bizzi A, Dell'Acqua F, Allin M, Walshe M, et al. Atlasing location, asymmetry and inter-subject variability of white matter tracts in the human brain with MR diffusion tractography. NeuroImage 39 2011; 54; 45-59.

Umarova RM, Nitschke K, Kaller CP, Kloppel S, Beume L, Mader I, et al. Predictors and signatures of recovery from neglect in acute stroke. Ann Neurol 2016; 79; 673-86.

Valero-Cabre A, Rushmore RJ, Payne BR. Low frequency transcranial magnetic stimulation on the posterior parietal cortex induces visuotopically specific neglect-like syndrome. Exp Brain Res 2006; 172; 14-21.

Vanbellingen T, Ottiger B, Pflugshaupt T, Mehrholz J, Bohlhalter S, Nef T, et al. The Responsiveness of the Lucerne ICF-Based Multidisciplinary Observation Scale: A Comparison with the Functional Independence Measure and the Barthel Index. Front Neurol 2016; 7; 152.

Vanbellingen T, Ottiger B, Maaijwee N, Pflugshaupt T, Bohlhalter S, Müri RM, et al. Spatial Neglect Predicts Upper Limb Use in the Activities of Daily Living. Cerebrovascular Diseases 2017; 44;

Vuilleumier P, Hester D, Assal G, Regli F. Unilateral spatial neglect recovery after sequential strokes. Neurology 1996; 46; 184-9.

WHO. World Medical Association Declaration of Helsinki Ethical Principles for Medical Research Involving Human Subjects. JAMA 2013; 310; 2191-2194.

Winters C, van Wegen EE, Daffertshofer A, Kwakkel G. Generalizability of the Maximum Proportional Recovery Rule to Visuospatial Neglect Early Poststroke. Neurorehabil Neural Repair 2017; 31; 334-342.

Woo NH, Nguyen PV. Protein synthesis is required for synaptic immunity to depotentiation. J Neurosci 2003; 23; 1125-32.

Zhou Q, Tao HW, Poo MM. Reversal and stabilization of synaptic modifications in a developing visual system. Science 2003; 300; 1953-7.

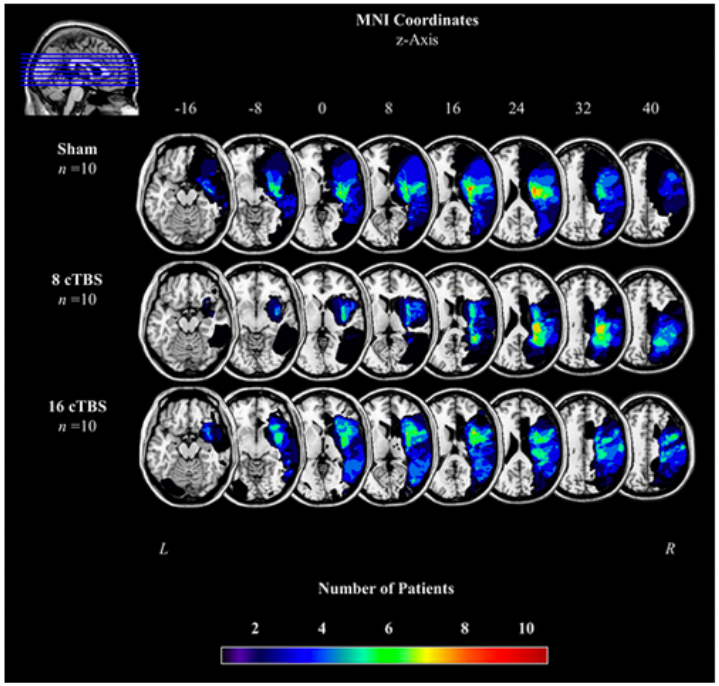

Figure 1- Lesion overlap maps of the 30 patients in the three stimulation conditions.
Lesion overlap maps of the 30 patients in the three stimulation conditions (sham stimulation, 8cTBS, 16cTBS). The color-coded legend indicates the number of patients with damage to a specific brain region. The lesion overlap maps are plotted on the CH2 template, as available in MRIcron (http://www.mccauslandcenter.sc.edu/crnl/chris-rordens-neuropsychology-lab). Axial slices are oriented according to the neurological convention. The z-position of each axial slice, in MNI coordinates, is indicated by the numbers at the top of the figure, and also depicted by the blue lines on the sagittal slice (top left of the figure).

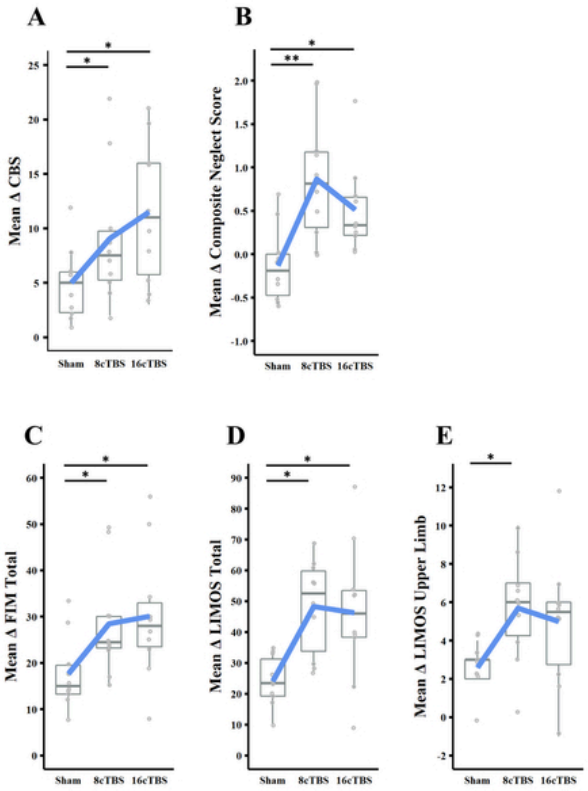

Figure 2 – Improvement between admission and discharge from neurorehabiliation.

(A) CBS improvement between admission to and discharge from neurorehabilitation (T0-T1). (B) Improvement in the neglect composite score between admission to and discharge from neu-rorehabilitation (T0-T1). (C, D, E) Improvement of the functional outcome (FIM Total, LIMOS Total and, with particular reference to arm involvement, LIMOS Upper Limb) between admis-sion to and discharge from neurorehabilitation. Results are shown as whisker plots; each box representing the upper to the lower quartiles with whiskers extending to the minimum and max-imum of 1.5 times the interquartile range, Mean values per group are indicated by the blue line and individual data by grey points. Asterisks represent significant post-hoc tests between the three stimulation conditions (sham, 8cTBS, 16cTBS; ** p < .01, * p < .05).

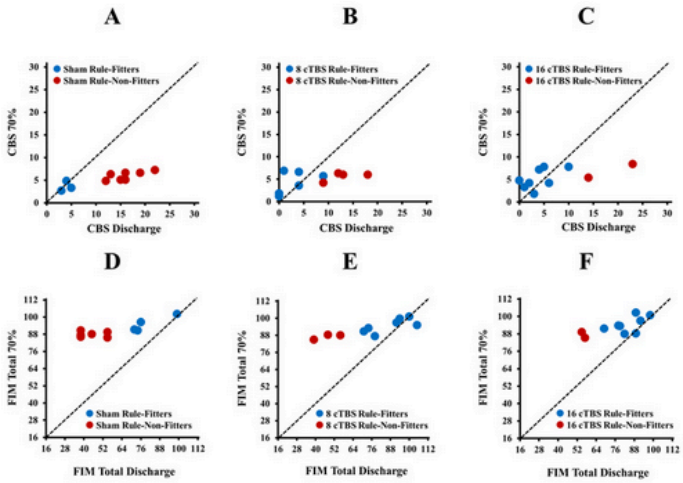

Figure 3 – Expected versus measured scores for CBS and FIM according the Proportional recovery rule.

Expected CBS scores according the Proportional recovery rule (i.e., recovery of ≈70% of the initial impairment, irrespective of therapy; y-axis), and measured CBS scores at discharge, i.e. before 3 months (x-axis), separately presented for the three stimulation groups. Hierarchical clustering revealed that only 30% of patients receiving sham stimulation fitted the predictions of the Proportional recovery rule at discharge (A). In contrast, 60 % of neglect patients undergoing 8cTBS trains (B), and 80% of neglect patients undergoing 16cTBS trains (C) already fitted the predictions of the Proportional recovery rule at discharge.

Expected FIM scores according the Proportional recovery rule (i.e., recovery of ≈70% of the initial impairment, irrespective of therapy; y-axis), and measured FIM scores at discharge (x-axis), separately presented for the three stimulation groups. Hierarchical clustering revealed that only 40% of neglect patients receiving sham stimulation fitted the predictions of the Proportional recovery rule (D). In contrast, 70 % of the neglect patients already fitted these predictions in the 8cTBS group (E), and 80% of the neglect patients in the 16cTBS condition (F). The dotted lines represent perfect predictions of the Proportional recovery rule (i.e., score predicted by the rule perfectly corresponding to the score measured at discharge at 3 months).

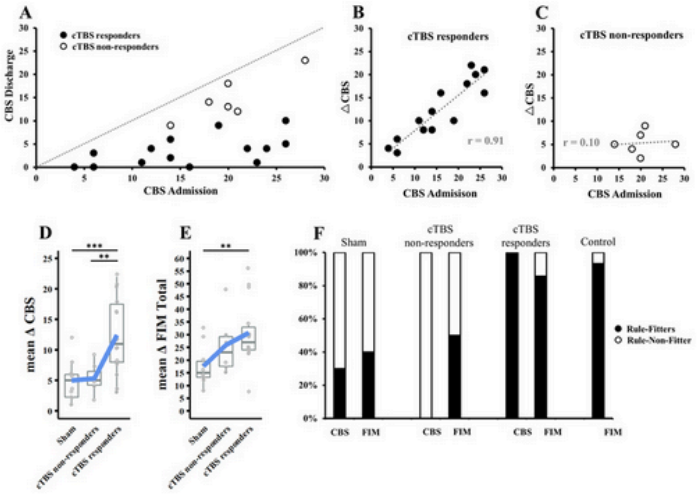

Figure 4 – Comparing cTBS responders and cTBS non-responders.

A. CBS scores at admission, plotted against CBS scores at discharge, for all neglect patients who received cTBS (i.e., 8cTBS and 16cTBS considered together); the dotted line represents the absence of change. Based on a hierarchical cluster analysis, patients were divided into cTBS responders and cTBS non-responders. B. In the group of cTBS responders, the severity of ne-glect at admission significantly correlated with the cTBS effects (in terms of ΔCBS); C. this was not the case in the group of cTBS non-responders. In cTBS responders, neglect recovery (D) and general functional outcome (E) were significantly improved. F. A higher proportion of fitters (as defined with respect to the Proportional recovery rule) was observed in the cTBS responder sub-group than in the sham group and in the cTBS non-responder subgroup, both concerning neglect severity (CBS) and general functional outcome (FIM). Results in Subplot A, B and C are shown as scatter plots; individual values of responders and non-responders are indicated in black, and white respectively. The grey line represents the correlation of the variables plotted on the x and y-axis. Results of subplots D and E shown as whisker plots; each box representing the upper to the lower quartiles with whiskers extending to the minimum and maximum of 1.5 times the in-terquartile range, Mean values per group are indicated by the blue line and individual data by grey points Asterisks represent significant post-hoc tests (*** p≤.001; ** p<.01).

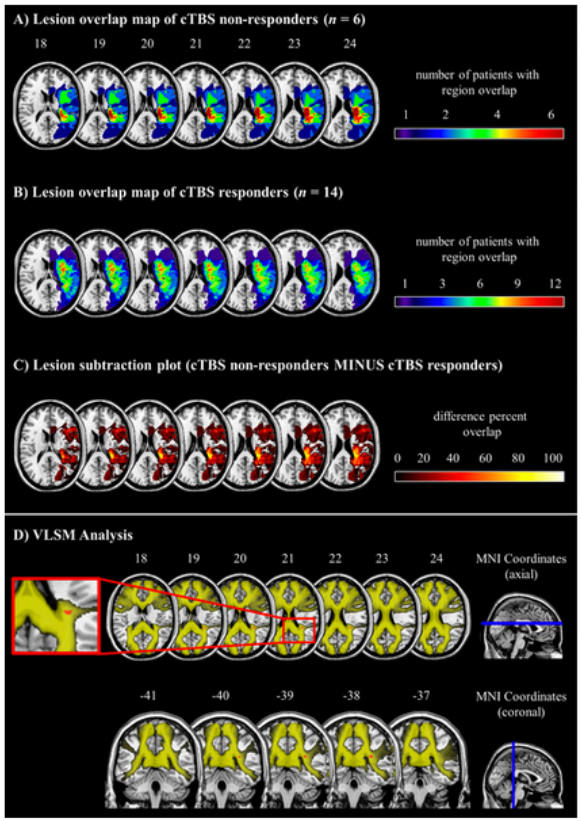

Figure 5 - Lesion overlap maps and results of the VLSM analysis comparing cTBS re-sponders and non-responders.
Lesion overlap maps in the subgroup of cTBS non-responders (A) and of cTBS responders (B). The colour-coded legend indicates the number of patients with damage to a specific brain region. C. Lesion subtraction plot (i.e., cTBS non-responders minus cTBS responders). The colour-coded legend indicates the difference percent overlap. The lesion overlap maps and the subtraction plot are represented on the CH2 template, as available in MRIcron (http://www.mccauslandcenter.sc.edu/crnl/chris-rordens-neuropsychology-lab). Axial slices are oriented according to the neurological convention. The z-position of each axial slice, in MNI coordinates, is indicated by the numbers at the top of the figure, and also depicted by the blue, horizontal lines on the sagittal slice (bottom right of the figure). D. Results of the VLSM analy-sis. Voxels that were significantly more often lesioned in cTBS non-responders are depicted in red (significance level $p < 0.05$, based on the Liebermeister test, FDR-corrected, 4000 permuta-tions). The corpus callosum and its projections are depicted in yellow, according to published probabilistic diffusion tensor imaging (DTI) tractography atlases (Rojkova et al., 2016; Thiebaut de Schotten et al., 2011); the probability for voxels to belong to the corpus callosum is set at >50% (i.e., above chance). The lesion cluster and the corpus callosum are displayed on the CH2 template, as available in MRIcron (http://www.mccauslandcenter.sc.edu/crnl/chris-rordens-neuropsychology-lab). The axial and coronal slices are oriented according to the neurological convention. The z-position of each axial and the y-position of each coronal slice, in MNI coordi-nates, is indicated by the numbers at the top of each slice, and is also depicted by the blue, hori-zontal lines on the sagittal slice (for axial slices) and by the blue, vertical lines on the sagittal slice (for coronal slices) at the bottom right of the figure. The significant lesion cluster (60 voxels) is located in the right, posterior part of the corpus callosum (MNI coordinates of the centre of mass of the cluster: 31, -39, 21).

Table 1. Demographic and clinical characteristics of neglect patients, at rehabilitation admission (baseline)

	Sham (n = 10)	8cTBS (n = 10)	16cTBS (n = 10)	P-value
Age	70.60 ± 11.44	67.80 ± 10.13	74.30 ± 10.23	.402
Sex (male/female)	7/3	5/5	6 /4	.684
MoCA score	13.80 ± 4.42	18.33 ± 3.61	16.89 ± 3.55	.050
Years of education	12.45 ± 2.99	9.70 ± 2.95	12.35 ± 5.60	.243
Handedness (right/left/ambidextrous)	9/1/0	9/1/0	9/0/1	.254
Time after stroke onset (days)	25.8 ± 11.26	26.8 ± 20.89	22.90 ± 10.34	.833
Length of rehabilitation stay (days)	53.90 ± 11.86	46.60 ± 13.57	59.80 ± 17.80	.149
Lesion volume (cm^3)	105.30 ± 112.24	79.101 ± 62.39	99.92 ± 83.55	.785
CST lesion load (%)	11.89 ± 10.14	9.59 ± 13.69	11.92 ± 13.53	.894
Jamar score (kg)	19.0 ± 13.53	20.2 ± 6.98	16.2 ± 12.38	.827
NSA score	8.5 ± 7.14	11.75 ± 6.18	13.0 ± 6.78	.612
NIHSS score	13.30 ± 7.28	10.44 ± 5.13	11.90 ± 6.32	.693
CBS score	17.50 ± 4.99	16.10 ± 6.79	18.3 ± 7.39	.744
Fluff Test score	11	9.7	9.4	.372
Two-Part-Picture-Test asymmetry score (near space)	.28	.14	.39	.080
Two-Part-Picture-Test asymmetry score (far space)	.35	.15	.33	.120
Bird Cancellation Test (CoC)	.33	.56	.35	.255
LIMOS Total score	84.51 ± 24.09	92.15 ± 23.63	94.33 ± 23.58	.629
LIMOS Upper Limb score	10.22 ± 3.76	10.80 ± 3.25	11.37 ± 4.28	.796
FIM score	41.30 ± 16.80	47.20 ± 19.11	48.70 ± 19.11	.634
Left visual field extension	67.00 ± 36.30	56.50 ± 38.81	57.50 ± 35.77	.784

All values are stated as mean ± standard deviation (SD). p-values refer to the results of the separate, univariate analyses of variance (ANOVAs), comparing the values between the three groups. Abbreviations: CBS: Catherine Bergego Scale; CoC: Center of Cancellation; CST: corticospinal tract; FIM: Functional Independence Measure; LIMOS: Lucerne ICF-based Multidisciplinary Observation Scale; MoCA = Montreal Cognitive Assessment; NIHSS = NIH Stroke Scale; NSA = Nottingham Sensory Assessment; left visual field extension measured on the horizontal meridian by means of Goldmann perimetry (isopter III/4).

Table 2. Clinical and demographic factors correlating with general functional outcome in neglect patients

	Mean	SD	Δ FIM r (P-value)	Δ LIMOS total r (P-value)	Δ LIMOS upper limb r (P-value)
Δ CBS	8.53	6.04	0.43 (0.02 *)	0.45 (0.01 *)	0.43 (0.02 *)
Age	70.87	10.62	-0.41 (0.03 *)	-0.19 (0.32)	-0.17 (0.37)
Years of Education	11.50	4.10	-0.27 (0.14)	-0.05 (0.81)	-0.24 (0.20)
Lesion Volume	94.77	86.12	-0.02 (0.93)	-0.10 (0.60)	-0.15 (0.43)
CST Lesion Load	11.13	12.17	-0.09 (0.66)	-0.13 (0.49)	-0.20 (0.28)
Length of Stay	53.43	15.14	0.08 (0.68)	-0.04 (0.84)	-0.17 (0.36)
Time Post Stroke	15.47	13.06	0.23 (0.22)	-0.02 (0.93)	-0.01 (0.96)
NIHSS	11.79	6.16	0.07 (0.73)	-0.08 (0.96)	-0.01 (0.95)
MoCA	16.25	4.23	0.01 (0.98)	0.42 (0.03 *)	0.23 (0.24)

Table 3. Results of the stepwise hierarchical regression analyses, with ΔFIM, ΔLIMOS, ΔLIMOS upper limb scores as dependent variables

	β	*SE*	*T*	*p*	*R2*	*F*	*p*
Δ FIM Model I					0.29	3.31	0.04
Δ CBS	0.45	0.34	2.58	0.02			
Age	-0.22	0.21	-1.21	0.24			
NIHSS	0.02	0.34	-0.09	0.93			
Δ FIM Model II					0.29	3.22	0.04
Δ CBS	0.45	0.35	2.51	0.02			
Age	-0.25	0.20	-1.46	0.16			
MoCA	-0.11	0.50	-0.62	0.54			
Δ LIMOS Model I					0.31	3.44	0.03
Δ CBS	0.37	0.57	2.1	0.047			
MoCA	0.32	0.92	1.79	0.087			
NIHSS	-0.11	0.59	-0.65	0.53			
Δ LIMOS Model II					0.31	3.62	0.03
Δ CBS	0.37	0.57	2.10	0.047			
MoCA	0.33	0.81	1.92	0.07			
Age	-0.05	0.33	-0.29	0.77			
Δ LIMOS upper limb Model I					0.24	4.19	0.03
Δ CBS	0.44	0.08	2.63	0.01			
CST lesion load	-0.23	0.04	-1.35	0.19			

Abbreviations: SE = Standard error; CBS = Catherine Bergego Scale; NIHSS = NIH Stroke Scale; MoCA = Montreal Cognitive Assessment.

Supplementary Material for

Theta burst stimulation in neglect after stroke:

functional outcome and response variability origins

CONTENT

SUPPLEMENTARY METHODS

The CONSORT Diagram

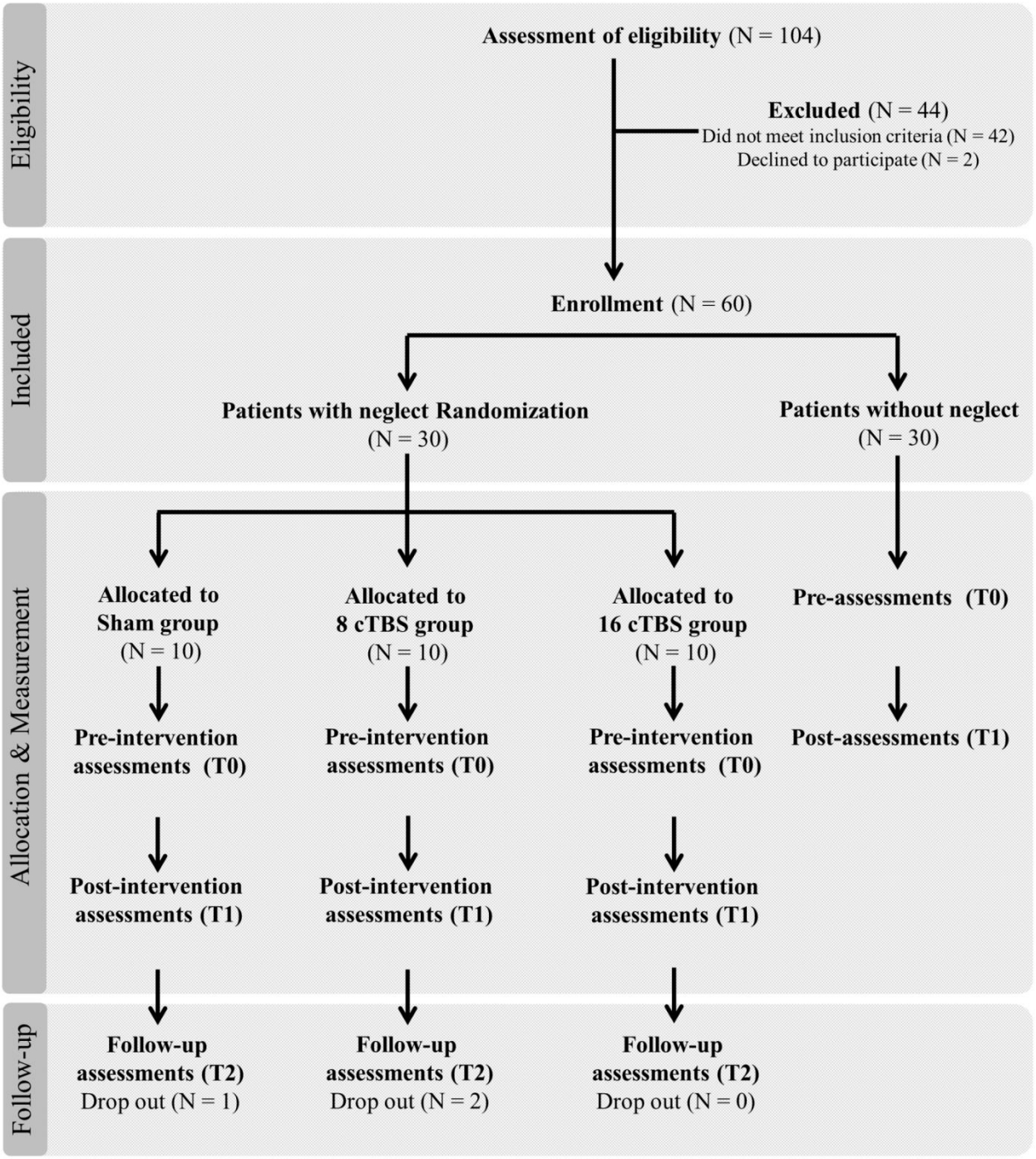

A priori sample size calculation

Analyses for the a priori computation of the required sample size were conducted with the G*Power 3 software (Faul *et al*., 2007; Faul *et al*. 2009). The probability of an alpha error was customarily set at .05 (2-tailed). The probability of a beta error was set as four times the probability of an alpha error, according to the recommendations by Cohen (1988) i.e., .20. This results in a power of .80. The expected effect size was calculated, on the results of our previous paper (Cazzoli, et al. 2012). Hereby, a model was calculated for a between factors ANOVA, with three groups of neglect patients (8 cTBS, 16 cTBS, sham stimulation) and two measurements (i.e. △CBS T0-T1, △CBS T1-T2). According previous paper a moderate to strong correlation between measurements was assumed (i.e., r = .30-0.50, according to the classification by Cohen, 1988). The computation yielded a required total sample size of 30 neglect patients (i.e., 10 patients per treatment group).

Secondary outcomes

The Fluff Test (Cocchini *et al*., 2001) is used to assess body representation in neglect patients. Hereby, twenty-four sticky notes are attached to the participants' body (trunk and thighs; 12 left, 12 right), and have to be removed with the eyes closed. In the present study, performance in this test, and hence body representational neglect severity, was measured in terms of the total number of removed sticky notes on the left side of the body.

In order to assess free visual exploration behaviour, we used the Two-Part-Picture-Test (Brunila *et al*., 2003), a commonly used screening tool for visuospatial neglect. In this test, the drawings of two room interiors are simultaneously presented side-to-side, and the patients are asked to describe the different items present in the drawings. Each of the two rooms interiors contains 10 items (i.e., 10 items within the left and 10 items within the right room interior drawing, respectively). Correctly named items are scored with one point each. An asymmetry score is then calculated, using the number of correct items on the left side divided by the total number of correct

items ($Asymmetry\ Score = \left(\frac{correct\ items\ left}{correct\ items\ total}\right)$; (Brunila *et al*., 2003). The test was conducted twice, i.e., once within the near space and once within the far space. For the near space, the drawings were shown at reading distance, on an A3-format sheet of paper, placed in landscape orientation. The sheet of paper was placed on the table in front of the patients, the line dividing the two room interior drawings being aligned with the patients' midsagittal axis. For the far space, the same drawings were presented on a 685 cm x 1215 cm flat screen (LED) monitor, at a distance of two meters from the patients, with the same alignment as for the near space.

In the Bird Cancellation Test, 64 targets (images of birds displayed as flying towards the participant) and 96 distractors (images of birds displayed as flying in other directions) were evenly distributed on a 685 cm x 1215 cm touch screen (Hopfner *et al*., 2015). The patients were comfortably seated at a distance of 0.5 meters from the touch screen. They were asked to identify and cancel only the targets, by tapping on them with a stick with a rubber tip, held with the right hand, allowing them to easily reach every point of the large touch screen. The centre of mass of the spatial distribution of correctly identified targets was calculated by means of the Centre of Cancellation (CoC) index (Rorden and Karnath, 2010).

The FIM is a standardized assessment of general functioning during the ADLs, including 18 items that are rated on a 7-point scale, concerning the amount of assistance needed by the patient: 1 = total assistance; 2 = maximal assistance; 3 = moderate assistance; 4 = minimal contact assistance; 5 = supervision or set-up; 6 = modified independence; and 7 = complete independence. The FIM consists of 13 motor (or physical) items and of 5 cognitive items. The total scores can range from 13 to 91 for the motor subscale, and from 5 to 35 for the cognitive subscale.

The LIMOS includes 7 chapters, overall incorporating 45 items: 1) Learning and applying knowledge, 2) General tasks and demands, 3) Communication, 4) Mobility, 5) Self-care, 6) Domestic life, and 7) Interpersonal interactions and relationships (for more details, see (Ottiger *et al*., 2015) (Vanbellingen *et al*., 2016). Every item is rated on a 5-point scale (1-5), so that the total

score can range from 45 to 225. The 5-point scale of the LIMOS is defined as follows: 1 = the patient is not able to fulfil a task or needs assistance up to 75 % (corresponding to "complete"); 2 = the patient is able to fulfil tasks with an assistance of 25 % to 75 % (corresponding to "severe"); 3 = the patient is able to fulfil tasks with an assistance of less than 25 % or under supervision (corresponding to "moderate"); 4 = the patient is able to fulfil tasks independently, but needs more time and/or auxiliary materials, aids (corresponding to "slight"); 5 = the patient is able to fulfil tasks independently (corresponding to "none").

The LIMOS upper limb consists of 5 items: lifting and carrying objects, fine hand use, hand and arm use, washing the upper body, as well as putting on and taking off clothes in the upper body. The total LIMOS upper limb score can thus range from 5 (totally dependent) to 25 (totally independent).

Lesion mapping and analysis

Lesion mapping

The borders of the lesions were manually delineated on every transverse slice of the patients' individual, high-resolution (voxel size=1mm^3) structural MRI scans (3 T MAGNETOM Skyra Siemens) by means of the MRIcron software ((Rorden *et al*., 2007); http://www.mccauslandcenter.sc.edu/crnl/chris-rordens-neuropsychology-lab). Lesion delineation was performed by an experienced collaborator, who was naïve with respect to the hypotheses of the study.

The lesions were manually delineated on T2-weighted scans. The scans and the delineated lesions were then mapped into MNI space by means of the Clinical Toolbox (Rorden *et al*., 2012) run in SPM 12 (https://www.nitrc.org/projects/clinicaltbx), applying enantiomorphic normalization ((Nachev *et al*., 2008); http://www.fil.ion.ucl.ac.uk/spm).

Lesion overlap, lesion-symptom mapping analyses, probabilistic white matter fibre tract disconnection analysis, and lesion volume determination

To carry out voxel-based lesion-symptom mapping (VLSM), the freely available NPM software (http://www.cabiatl.com/mricro/npm/) was used. The lesions of the cTBS responders subgroup were compared with those of the cTBS non-responders subgroup (see Methods section) by means of the Liebermeister test. Only voxels that were lesioned in at least 20% of the patients were included in the analysis. The significance threshold was adjusted by means of a false discovery rate approach (FDR criterion = 0.05). Multiple comparisons were controlled for using a permutation-based thresholding (Kimberg *et al*., 2007), applying 4000 iterations, as proposed by Medina and colleagues (Medina *et al*., 2010).

Lesion overlap maps were plotted on the CH2 template, as available in MRIcron (http://www.mccauslandcenter.sc.edu/crnl/tools). Lesion volume was computed by means of the corresponding function implemented in MRIcron (http://www.mccauslandcenter.sc.edu/crnl/tools).

In order to ascertain whether the corpus callosum would be affected by the lesion cluster identified by means of the VLSM analyses, we performed a probabilistic analysis using the Tractotron software, as a part of the BCBtoolkit ((Foulon *et al*., 2018) http://www.toolkit.bcblab.com). First, we converted all significant voxels identified by the VLSM analysis into a binary mask. Then, by means of the Tractotron software, we mapped this mask onto the probabilistic tractography reconstruction of the corpus callosum, based on published diffusion tensor imaging (DTI) tractography atlases (Foulon *et al*., 2018; Rojkova *et al*., 2016; Thiebaut de Schotten *et al*., 2011). For each voxel in the MNI space, the atlases provide the probability to belong to a specific white matter tract, in this case the corpus callosum. Accordingly, the results of the analysis with the Tractotron software provide the probability of disconnection of the corpus callosum in terms of the lesioned voxel with the highest percentage probability value.

In order to estimate corticospinal lesion load, we adopted a similar probabilistic approach, using the right corticospinal tract map included in the above-mentioned probabilistic DTI tractography atlases (Rojkova *et al*., 2016; Thiebaut de Schotten *et al*., 2011). For each individual, normalized lesion map of the patients, we computed the number of voxels overlapping with this map (the probability of voxels belonging to the right corticospinal tract being set at > 50%, i.e., above chance level).

SUPPLEMENTARY RESULTS

Supplementary Figures

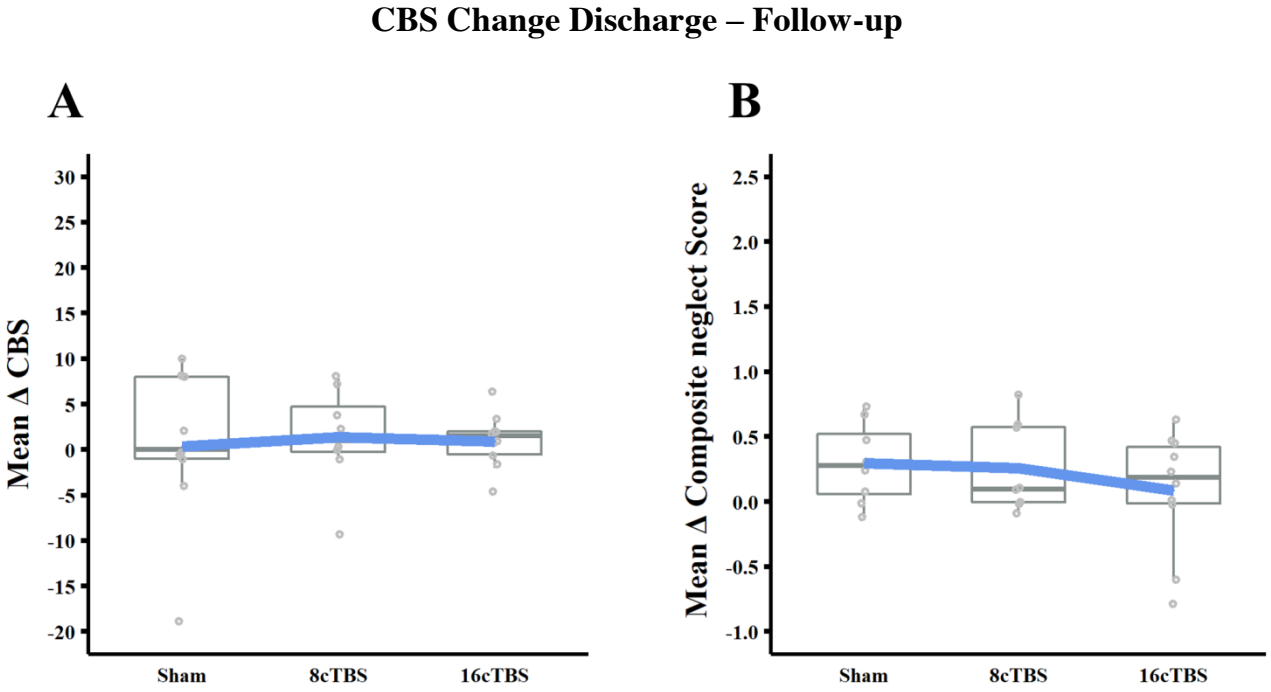

Supplementary Figure 1. (A) CBS improvement between discharge from neurorehabilitation and follow-up assessment three months later (T1-T2), for the three stimulation conditions. **(B)** Improvement in the neglect composite score between discharge from neurorehabilitation and follow-up assessment three months later (T1-T2), for the three stimulation conditions. Results are shown as whisker plots; each box representing the upper to the lower quartiles with whiskers extending to the minimum and maximum of 1.5 times the interquartile range, Mean values per group are indicated by the blue line and individual data by grey points.

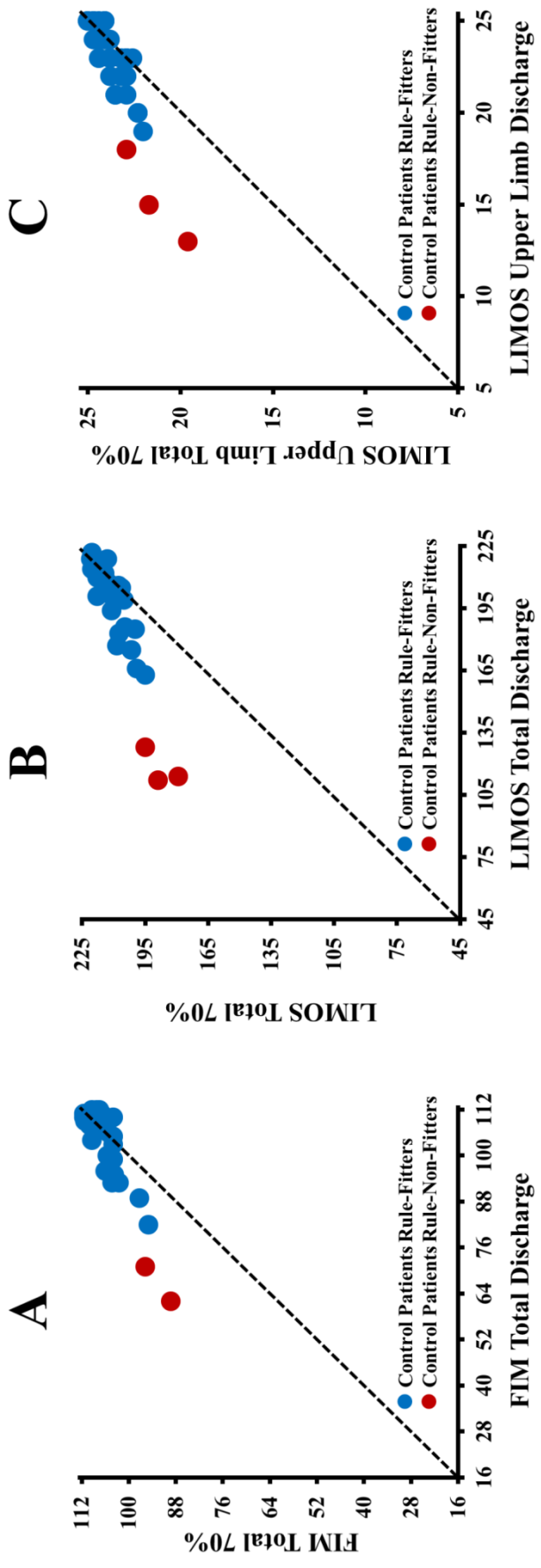
A
FIM Total 70%
FIM Total Discharge
Control Patients Rule-Fitters
Control Patients Rule-Non-Fitters
112
100
88
76
64
52
40
28
16
16 28 40 52 64 76 88 100 112
B
LIMOS Total 70%
LIMOS Total Discharge
225
195
165
135
105
75
45
45 75 105 135 165 195 225
C
LIMOS Upper Limb Total 70%
LIMOS Upper Limb Discharge
25
20
15
10
5
5 10 15 20 25

Supplementary Figure 2 Expected values according the Proportional recovery rule (i.e., recovery of ≈70% of the initial impairment, irrespective of therapy; y-axis), and observed values at discharge (x-axis), concerning functional outcome, in the control group of RHD patients with right-hemispheric lesions but not neglect, as measured by FIM **(A)**, LIMOS **(B)**, and LIMOS upper limb **(C)**. The colour-code indicates the allocation to one of the two subgroups defined by means of hierarchical clustering. 93% of patients followed the predictions of the Proportional recovery rule for the FIM score, and 90% of patients for both the LIMOS and the LIMOS Upper Limb scores

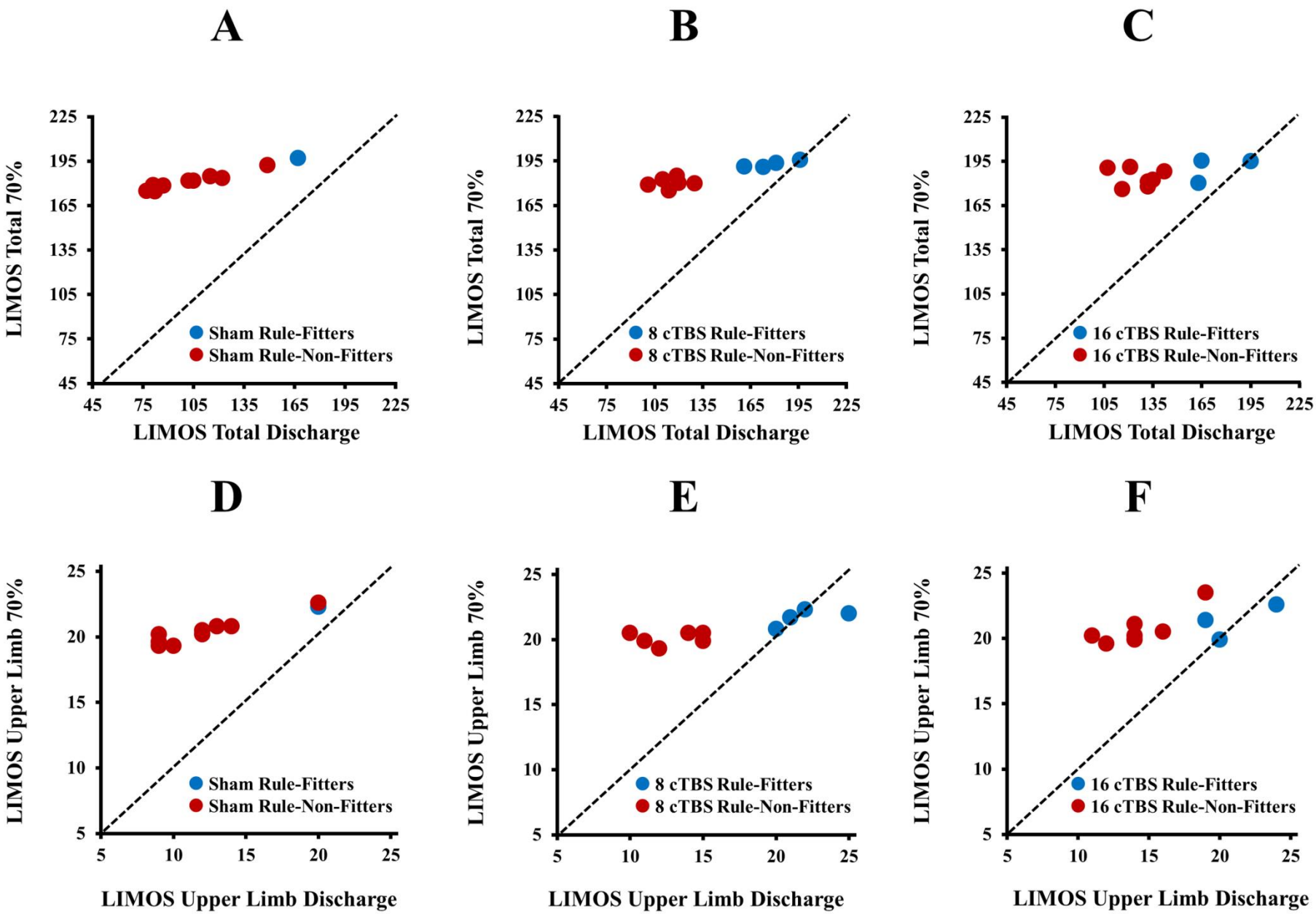
A
B
C
D
E
F
LIMOS Total 70%
LIMOS Upper Limb 70%
LIMOS Total Discharge
LIMOS Upper Limb Discharge
Sham Rule-Fitters
Sham Rule-Non-Fitters
8 cTBS Rule-Fitters
8 cTBS Rule-Non-Fitters
16 cTBS Rule-Fitters
16 cTBS Rule-Non-Fitters
45
75
105
135
165
195
225
5
10
15
20
25

Supplementary Figure 3

Upper row: Expected LIMOS scores, according the Proportional recovery rule (i.e., recovery of ≈70% of the initial impairment, irrespective of therapy; y-axis), plotted against the observed LIMOS scores at discharge (x-axis), presented for the three stimulation groups. Hierarchical clustering revealed that 10% of neglect patients receiving sham stimulation followed the predictions of the Proportional recovery rule **(A)**, whereas this was the case for 40% of the neglect patients in the 8cTBS group **(B)**, and for 30 % of the neglect patients in the 16cTBS group **(C)**.

Lower row: Expected LIMOS upper limb scores, according the Proportional recovery rule (i.e., recovery of ≈70% of the initial impairment, irrespective of therapy; y-axis), plotted against the observed LIMOS upper limb scores at discharge (x-axis), presented for the three stimulation groups. Hierarchical clustering revealed that 10% of neglect patients receiving sham stimulation followed the predictions of the Proportional recovery rule **(D)**, whereas this was the case for 40% of the neglect patients in the 8cTBS group **(E)**, and for 30 % of the neglect patients in the 16cTBS group **(F)**.

The dotted lines represent perfect predictions of the Proportional recovery rule (i.e., score predicted by the rule perfectly corresponding to the score measured at discharge).

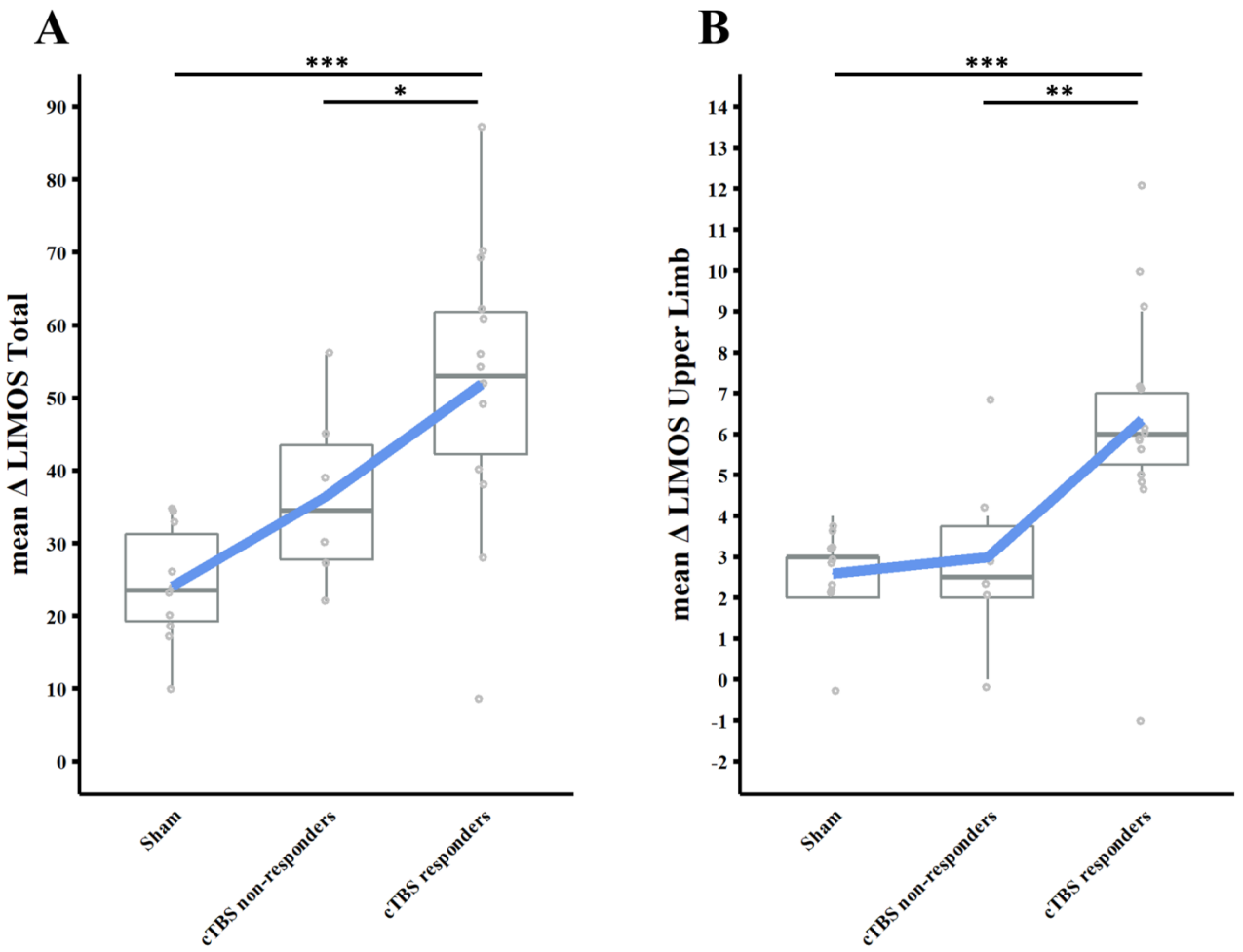

Supplementary Figure 4

Patients receiving cTBS (i.e., 8cTBS and 16cTBS considered together) were divided into two subgroups based on a hierarchical cluster analysis, i.e., cTBS responders and cTBS non-responders. The improvement in the LIMOS total score between admission and discharge from neurorehabilitation (T0-T1) differed significantly between cTBS responders and the sham group **(A)**. Concerning the LIMOS upper limb score, cTBS responders showed a significantly higher improvement than cTBS non-responders and sham **(B)**. Results are shown as whisker plots; each box representing the upper to the lower quartiles with whiskers extending to the minimum and maximum of 1.5 times the interquartile range, Mean values per group are indicated by the blue line and individual data by grey points. Asterisks indicate significant post-hoc tests (*** $p \leq .001$, ** $p \leq .01$, * $p < .05$).

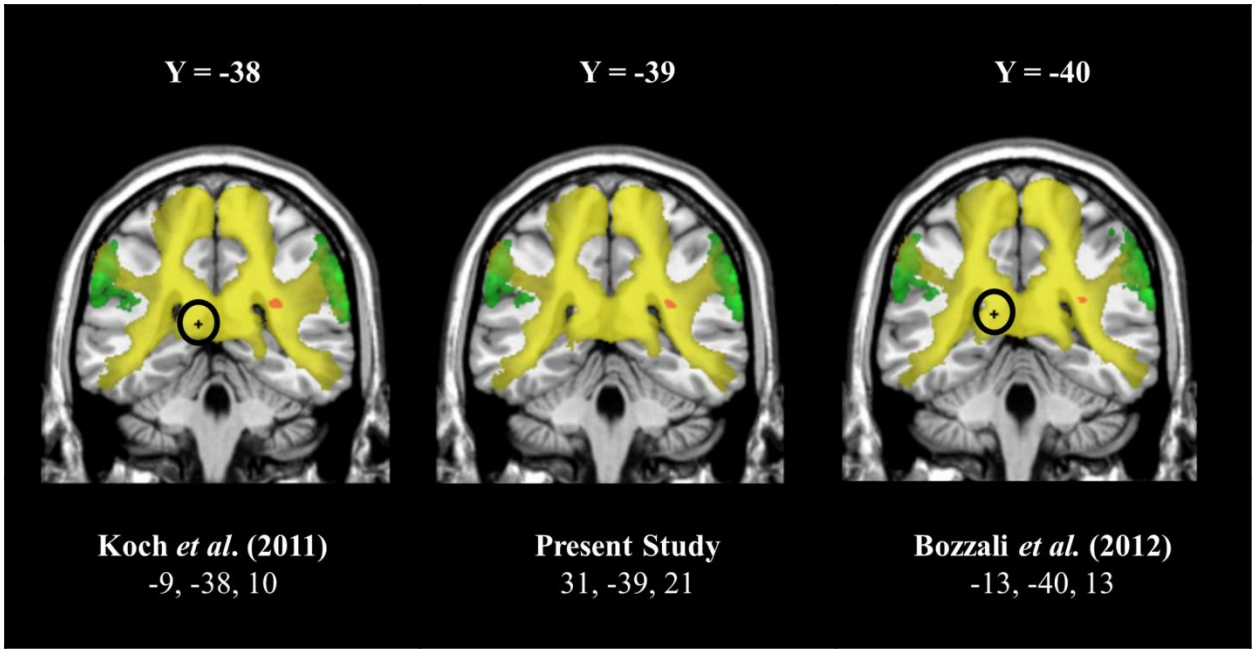

Supplementary Figure 5

The cluster of voxels that were significantly more often lesioned in cTBS non-responders than in cTBS responders is depicted in red, according to our Voxel-based Lesion-Symptom Mapping analysis (VLSM; see main body of the text for details). The black cross in the left panel of the figure indicates an area within the left corpus callosum (forceps major) whose fractional anisotropy is significantly associated with interhemispheric inhibition mechanisms, as assessed by transcranial magnetic stimulation (TMS) over the right posterior parietal cortex (Koch *et al*., 2011). The black cross in the right panel of the figure indicates a region of the posterior corpus callosum whose fractional anisotropy is associated with neglect severity, as assessed by the Behavioural Inattention Test (Bozzali *et al*., 2012).

The corpus callosum and its projections are depicted in yellow, according to published probabilistic diffusion tensor imaging (DTI) tractography atlases (Rojkova *et al*., 2016; Thiebaut de Schotten *et al*., 2011). The inferior parietal lobule is depicted in green, according to Caspers and colleagues ((Caspers *et al*., 2008); all seven cytoarchitectonic areas together, i.e., areas PF, PFcm, PFm, PFop, PFt, PGa, and PGp), as implemented in the Jülich Histological Atlas included in FSL (Jenkinson *et al*., 2012). The probability for voxels to belong to the respective structures is set at >50% (i.e.,

above chance).

The lesion cluster, the corpus callosum, and the inferior parietal lobule are displayed on the CH2 template, as available in MRIcron (http://www.mccauslandcenter.sc.edu/crnl/chris-rordens-neuropsychology-lab). The coronal slices are oriented according to the neurological convention. The y-position of each slice, in MNI coordinates, is indicated by the numbers at the top of the figure.

Supplementary Tables

Supplementary Table 1 – Input data and predictions of the Maugeri Model (Scrutinio *et al.*, 2017)

Group	Age	Sex	Time since stroke	FIM Motor Admission score	FIM Cognition Admission score	Probability FIM Motor Discharge	Actual FIM Motor Discharge
			(in days)			*(in %)*	
sham	83	m	14	27	17	13.30	44
	59	m	21	26	20	22.40	66
	70	m	30	19	18	4.80	30
	77	m	8	14	12	2.90	29
	45	f	14	25	20	33.90	58
	72	f	13	22	23	13.50	35
	80	m	7	65	27	100.00	83
	65	m	15	19	13	7.00	25
	77	m	7	46	19	78.30	68
	77	f	11	17	12	3.90	23
8 cTBS	52	m	61	16	16	2.10	65
	58	m	53	23	24	8.00	55
	83	f	12	13	11	1.70	26
	79	f	10	17	20	5.50	32
	70	m	8	36	17	50.40	56
	66	f	8	60	28	98.20	81
	55	m	12	45	19	85.30	88
	72	m	7	17	18	6.90	41
	70	f	7	49	23	89.50	74
	73	f	5	61	24	97.80	79
16 cTBS	80	m	15	69	25	100.00	76
	64	m	7	16	10	5.40	41
	52	m	34	38	28	65.60	78
	82	m	11	41	15	52.20	67
	80	m	17	63	24	100.00	81
	79	f	8	27	19	19.00	58
	67	f	11	16	19	6.60	64
	81	m	8	25	13	11.00	78
	74	f	13	26	15	14.60	45
	84	f	17	39	17	41.40	62

Group	Age	Sex	Time since stroke	FIM Motor Admission score	FIM Cognition Admission score	Probability FIM Motor Discharge	Actual FIM Motor Discharge
			(in days)			*(in %)*	
control	64	f	5	46	17	95.20	72
	45	m	7	77	22	100.00	89
	86	f	5	76	22	100.00	80
	52	f	10	86	32	100.00	90
	47	m	14	91	32	100.00	91
	57	m	18	69	29	100.00	89
	68	m	7	89	35	100.00	89
	80	f	6	47	22	94.10	72
	58	m	26	75	23	100.00	85
	66	m	8	77	30	100.00	88
	54	f	24	91	30	100.00	91
	84	f	11	73	30	100.00	78
	54	m	6	83	32	100.00	89
	45	f	10	91	26	100.00	91
	64	m	9	72	35	100.00	88
	81	m	9	40	24	85.50	58
	46	m	7	78	32	100.00	89
	81	m	7	23	17	29.80	42
	56	m	6	77	34	100.00	91
	80	f	7	71	26	100.00	80
	47	m	6	79	31	100.00	91
	85	f	8	73	29	100.00	79
	54	m	21	76	25	100.00	90
	63	m	9	91	33	100.00	91
	79	m	0	72	20	100.00	81
	63	f	15	73	26	100.00	89
	33	f	13	86	33	100.00	91
	80	m	21	81	31	100.00	89
	27	f	16	78	33	100.00	91
	57	m	4	86	32	100.00	91

REFERENCES

Bozzali M, Mastropasqua C, Cercignani M, Giulietti G, Bonni S, Caltagirone C, et al. Microstructural damage of the posterior corpus callosum contributes to the clinical severity of neglect. PLoS One 2012; 7.

Brunila T, Jalas M, Lindell JA, Tenovuo O, Hamalainen H. The two part picture in detection of visuospatial neglect. Clin Neuropsychol 2003; 17; 45-53.

Caspers S, Eickhoff S, Geyer S, Scheperjans F, Mohlberg H, Zilles K, et al. The human inferior parietal lobule in stereotaxic space. Brain Structure and Function 2008; 212; 481-495.

Cocchini G, Beschin N, Jehkonen M. The fluff test: a simple task to assess body representational neglect. Neuropsychological Rehabilitation 2001; 11; 17-31.

Cohen J . Statistical power analysis for the behavioral sciences. New York, NY: Routledge Academic 1988.

Faul, F., Erdfelder, E., Lang, A.-G., Buchner, A. (2007). G*Power 3: A flexible statistical power analysis program for the social, behavioral, and biomedical sciences. Behavior Research Methods 2007; 39; 175-191.

Faul F, Erdfelder E, Buchner A, Lang, AG. Statistical power analyses using G*Power 3.1: Tests for correlation and regression analyses. Behavior Research Methods 2009; 41; 1149-1160.

Foulon C, Cerliani L, Kinkingnéhun S, Levy R, Rosso C, Urbanski M, et al. Advanced lesion symptom mapping analyses and implementation as BCBtoolkit. GigaScience 2018; 7;

Hopfner S, Cazzoli D, Müri RM, Nef T, Mosimann UP, Bolhlhalter S, et al. Enhancing treatment effects by combining continuous theta burst stimulation with smooth pursuit training. neuropschologia 2015; 74; 145-51.

Jenkinson M, Beckmann, CF, Behrens T, Woolrich, MW, Smith S. FSL. NeuroImage 2012; 62; 782-790.

Kimberg DY, Coslett HB, Schwartz MF. Powerinvoxel- based lesion-symptommapping. J. Cogn.Neurosci. 2007; 19; 1067-1080.

Koch G, Cercignani M, Bonni S, Giacobbe V, Bucchi G, Versace V, et al. Asymmetry of parietal interhemispheric connections in humans. J Neurosci 2011; 31; 8967-75.

Medina J, Kimberg DY, Chatterjee A, Coslett HB. Inappropriate usage of the Brunner–Munzel test in recent voxel-based lesion-symptom mapping studies. Neuropsychologia 2010; 48; 341-343.

Nachev P, Coulthard E, Jäger HR, Kennard C, Husain M. Enantiomorphic normalization of focally lesioned brains. NeuroImage 39 2008; 39; 1245-1226.

Ottiger B, Vanbellingen T, Gabriel C, Huberle E, Koenig-Bruhin M, Pflugshaupt T, et al. Correction: Validation of the New Lucerne ICF Based Multidisciplinary Observation Scale (LIMOS) for Stroke Patients. PLoS One 2015a; 10.

Rojkova K, Volle E, Urbanski M, Humbert F, Dell'Acqua F, Thiebaut de Schotten M. Atlasing the frontal lobe connections and their variability due to age and education: a spherical deconvolution tractography study. Brain Structure and Function 2016; 221; 1751-1766.

Rorden C, Karnath HO, Bonilha L. Improving Lesion–Symptom Mapping. Journal of Cognitive Neuroscience 2007; 19; 1081-1088.

Rorden C, Karnath HO. A simple measure of neglect severity. Neuropsychologia 2010; 48; 2758-2763.

Rorden C, Bonilha L, Fridriksson J, Bender B, Karnath HO. Agespecific CT and MRI templates for spatial normalization. NeuroImage 2012; 61; 957-965.

Scrutinio D, Lanzillo B, Guida P, Mastropasqua F, Monitillo V, Pusineri M, et al. Development and Validation of a Predictive Model for Functional Outcome After Stroke Rehabilitation: The Maugeri Model. Stroke 2017; 48; 3308-3315.

Thiebaut de Schotten M, Ffytche DH, Bizzi A, Dell'Acqua F, Allin M, Walshe M, et al. Atlasing location, asymmetry and inter-subject variability of white matter tracts in the human brain with MR diffusion tractography. NeuroImage 39 2011; 54; 45-59.

Vanbellingen T, Ottiger B, Pflugshaupt T, Mehrholz J, Bohlhalter S, Nef T, et al. The Responsiveness of the Lucerne ICF-Based Multidisciplinary Observation Scale: A Comparison with the Functional Independence Measure and the Barthel Index. Front Neurol 2016; 7; 152.